Chem Soc Rev

REVIEW ARTICLE

View Article Online
View Journal | View Issue

Cite this: *Chem. Soc. Rev.*, 2023, 52, 8059

Heterogenization of molecular catalysts within porous solids: the case of Ni-catalyzed ethylene oligomerization from zeolites to metal–organic frameworks

Rémy Rajapaksha, Partha Samanta, Elsje Alessandra Quadrelli and Jérôme Canivet *

Received 30th May 2023

DOI: 10.1039/d3cs00188a

rsc.li/chem-soc-rev

The last decade has seen a tremendous expansion of the field of heterogenized molecular catalysis, especially with the growing interest in metal–organic frameworks and related porous hybrid solids. With successful achievements in the transfer from molecular homogeneous catalysis to heterogenized processes come the necessary discussions on methodologies used and a critical assessment on the advantages of heterogenizing molecular catalysis. Here we use the example of nickel-catalyzed ethylene oligomerization, a reaction of both fundamental and applied interest, to review heterogenization methodologies of well-defined molecular catalysts within porous solids while addressing the biases in the comparison between original molecular systems and heterogenized counterparts.

1. Introduction

Beyond an historical dichotomy, the frontier is continuously blurring between homogeneous catalysis, where a typically single atom in the same phase as the substrate is responsible of the catalytic transformation, and heterogeneous catalysis, where the cooperation between several surface atoms, in a separate phase than the substrate, is typically at the origin of substrate activation and transformation.

Using heterogenized molecular species enables to isolate active sites from each other and, as a consequence, prevents them from aggregating or interacting with one another, which could lead to the catalyst deactivation or undesired reactivity.[1–5]

Univ. Lyon, Université Claude Bernard Lyon 1, CNRS, IRCELYON – UMR 5256, 2 Av. Albert Einstein, 69626 Villeurbanne, France.
E-mail: jerome.canivet@ircelyon.univ-lyon1.fr

Rémy Rajapaksha

After studying chemistry engineering at CPE Lyon, Rémy Rajapaksha worked during his PhD on two types of porous supports, Metal–Organic Frameworks (MOFs) and Porous Organic Polymers (POPs), with bipyridyl coordination sites, under the direction of Dr Jérôme Canivet and Dr Elsje Alessandra Quadrelli at IRCELYON. His thesis work focused on nickel coordination chemistry at bipyridyl sites within MOF and POP structures in order to obtain isolated active sites. The synthesized catalysts were studied in the ethylene dimerization reaction. After obtaining his PhD from the University of Lyon in 2022, Rémy Rajapaksha joined Elkem Silicones – Lyon, in the Upstream team, as a research engineer.

Partha Samanta

Partha Samanta completed his BSc degree in 2011 and MSc degree in 2013 from the University of Calcutta and IIT Kharagpur, respectively. Then, he joined the research group of Dr Sujit K. Ghosh at IISER Pune to pursue his doctoral studies. In 2019, he obtained a PhD degree and then he joined IRCELYON as postdoctoral fellow with Dr Jerome Canivet, where he worked on heterogeneous catalysts for important organic transformations. And currently, he is working with Dr Daniel Maspoch at ICN2 (Barcelona, Spain) as postdoctoral researcher, and his research interest is focused on the Clip-off chemistry of reticular materials.

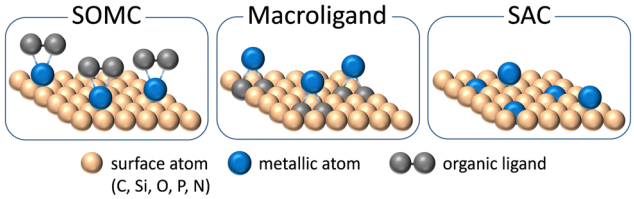

Fig. 1 Schematic representation of selected differences in designing heterogeneous single-site catalysts through the concepts of SAC, SOMC and macroligands.

Moreover, the site isolation changes the interactions at play during substrate activation on the heterogeneous catalyst, leading to unprecedented reactivities which can be understood in the light of organometallic chemistry mechanisms.[6–10]

The usefulness of mobilizing organometallic chemistry mechanisms in single-site heterogeneous catalysts is particularly pertinent for catalysts baring organic-based ligand-like moieties in their first coordination sphere since the metal–ligand environment is a key descriptor of the catalyst performance in organometallic chemistry.

The heterogenization of ligand-bearing metal-centered molecular catalysts can be achieved by grafting organometallic precursors on oxide surface. This strategy, also known as Surface Organometallic Chemistry (SOMC, Fig. 1),[11–15] gave access to well-defined isolated sites derived from molecular organometallic counterparts. Beyond the simple heterogenization, the SOMC strategy has already proven to lead in some cases to unique reactivity not accessible by any other molecular analogue, including enzymes and organometallics.[16]

More recently, the concept of porous macroligands proposed a variation of the SOMC approach in the field of single-site catalysts (Fig. 1).[17–19] Here a porous organic or hybrid organic–inorganic polymer, made with coordinating monomers like bipyridine derivatives, is defined and used as a solid ligand for the active metal cations. Macroligands include porous solids among periodic mesoporous organosilica (PMO), metal–organic frameworks (MOF) and porous organic polymers (POP).[20] The macroligand strategy lies in the derivatization of traditional organic ligand in coordination complexes, like bipyridine or triphenylphosphine, with functional groups such as carboxylic acids or polymerizable vinyl groups for subsequent reticulation in carboxylate-based MOF or in POP, respectively. In macroligands, the molecular catalyst is self-supported in the porous framework, minimizing possible detrimental interactions. Moreover, the nature of porous macroligands allows for an unprecedented site density, in catalytic sites per mass, since no bulk matter remains unused, unlike in traditional grafted siliceous materials.

Porous macroligands like MOF and POP already account for a wide variety of metal–ligand combinations for catalytic applications ranging from fine chemical synthesis to energy.[21–27] Such as for homogeneous and heterogeneous catalysts in general, the evolution of the heterogenized molecular catalyst during catalysis has to be scrutinized, especially in the well-documented case of highly reactive palladium complexes prompt to form clusters and particles, as well as prompt to release single-atom from aggregates, and showing high activity even at so-called homeopathic level.[28–31] Indeed, the retention of the molecular nature of the active site, *i.e.* coordination and structure, and the accessibility to substrates molecules when immobilized are key issues to be addressed. If confirmed, this allows for mechanistic studies at the molecular level following both computational and experimental methodologies from molecular science.[32–36] Furthermore, the electronic effect of the support on the active site dramatically affects its reactivity.[18,19] Therefore, the challenge remains to disentangle the electronic effect resulting from embedding the complex within the macroligand structure from the effect due to the confinement within macroligand's pores.

Since the early 2000s, a novel concept in heterogeneous catalysis appeared with the single atom catalysts (SAC) described as isolated single metal atoms or cations either embedded or supported on solid surfaces (oxide, metal,

Elsje Alessandra Quadrelli

Elsje Alessandra Quadrelli is director of research in chemistry from the French National Centre for Scientific Research, CNRS, at the IRCELYON laboratory. Her research focuses on organometallic mechanisms for grafting catalytically active transition metals or for growing thin films by atomic layer deposition (ALD) on surfaces (Silica, MOFs and silicon wafer substrates). Her current main target reaction is CO_2 reduction.

Jérôme Canivet

Jérôme Canivet was appointed CNRS researcher at the IRCELYON in 2010. He works at developing innovative catalytic processes for sustainable fine chemicals and energy. His research topics range from C–C coupling to asymmetry, photocatalysis and green fuels. In 2018, he received the Young Investigator Award from the Catalysis Division of the French Chemical Society for creating trends reducing the gap between homogeneous and heterogeneous catalysis. He further aims at exploiting the confinement of molecular catalytic systems into porous structures for the improvement of their catalytic activity and selectivity, and he is coordinating cooperative projects on this topic.

graphene or polymer, Fig. 1).[37–40] At the same time, the SAC concept constitutes a proximal yet distinct class of catalyst with respect to single-site catalysts of interest here if we follow Copéret and Korzyński classification: while single-site catalyst, a concept applicable to homogeneous and heterogeneous catalyses, is centered on the reactivity of well-defined isolated active sites, SAC are mostly defined by textural properties of individual atoms in a surface rather than by the coordination environment or nature of the bonding between the metal and the support (Fig. 1).[8]

The SAC concept therefore implies no (or weak) influence of other atoms in the first coordination sphere of grafted metal atom beyond the metal to surface bonds (such as M–O or M–C bonds at oxide or carbon surface respectively), while typically at least one coordinated organic molecule, which is absent in SAC systems, directly influences the electronic and/or steric properties of the grafted metal complex in SOMC or macroligand strategies though M–X bonds where X = C, O, N, P, S. Therefore the SAC systems, as well as the similarly ligand free catalysts that can be obtained by the thermolytic molecular precursor method,[41,42] are beyond the scope of this review, and will only be sporadically mentioned if they lead to performing materials against whose performance the performance of the SOMC or macroligand-based materials can be compared and contrasted.

In summary, we aim here at focussing on approaches directly influencing the ligand-based coordination environment of heterogenized single-site catalysts. The support described as an extended solid ligand for the active metal would allow direct comparison between heterogenized and homogeneous analogues beyond the practical advantages of using solid catalyst like easy separation from the catalysis medium and recycling. For a clear overview on the scope and limitations of molecular catalyst heterogenization, it is essential to focus on molecular catalytic application that has been extensively studied and documented. Furthermore, this application should be of industrial relevance, with particular attention given to sustainability with the use of earth-abundant active metal catalysts. The overall sustainability of a catalytic process can also be improved by the recycling of the heterogenized catalyst and the easy separation achieved. The absence of active species leaching and the high accessibility of active sites within solid supports can give access to the full productivity of the catalyst without diffusional limitation.[43]

In this review we aim at highlighting the perspectives offered by heterogenized molecular catalysts compared to homogeneous counterparts using the prism of the nickel-catalyzed ethylene oligomerization as widely studied and industrially relevant reaction.

2. Tailor-made nickel-based molecular catalyst for ethylene oligomerization

Ethylene α-oligomers are typically used in copolymerization with ethylene to modulate the properties of polyethylene. The recent increase of the availability of shale gas makes economically appealing to produce selectively α-oligomers or linear alpha-olefins (LAO) directly from ethylene. Industrial processes of ethylene oligomerization towards LAO rely mainly on titanium-, chromium-, zirconium- and nickel-based catalysis.[44,45]

Two types of mechanisms have been highlighted for ethylene oligomerization:

– a cycle of activation/coordination/insertion/elimination and/or propagation (also called Cossee–Arlman mechanism),[46,47]

– a cycle of coordination/oxidative coupling/metallacycle intermediate/elimination and/or propagation (also called metallacycle mechanism).[48,49]

In the case of a Cossee–Arlman mechanism, which has been demonstrated to be the most plausible for the nickel-catalysed reaction,[50] either metal halide (like nickel dihalide or titanium chloride) or metal hydride (like nickel hydride) complexes are typically used. Metal hydride complexes readily react with ethylene without prior activation.[51] In contrast, metal halide complexes, which are among the easiest to synthesize and the most stable, required an activation step in order to obtain the catalytically active species for ethylene oligomerization. This step typically involves an alkyl-aluminum activator (also called co-catalyst) which subtracts halides and subsequently generates the active metal alkyl species.

The important role of nickel in catalysis and its development as alternative to platinum group metals (PGM) during the last decades was already comprehensively reviewed.[52–57]

Beyond its acknowledged sustainability due to its large abundance and reduced cost compared to PGM,[58] nickel presents advantageous intrinsic electronic properties when dealing with C–C bond formation. Indeed, as compared to palladium and platinum, nickel–carbon bonds show the weakest dissociation energy which makes Ni–C intermediates highly reactive.[59,60]

The proliferation of catalytic systems based on molecular nickel species benefited to the field of polymer chemistry.[61–65] As of interest here, molecular nickel catalysts are well-known to oligomerize ethylene, among other olefins such as propylene and butene.[66,67]

Linked to its high reactivity, nickel catalysis often proceeds though a wide number of parallel pathways and elementary steps which multiplies the number of active intermediates.[68,69]

The reactivity of nickel species is highly dependent to their coordination sphere which makes the design of ligand in molecular catalysts crucial to obtained the desired product.[70,71] In terms of ligation, the *cis*-coordination of tetracoordinated Ni(II) sites is shown to favor migratory insertion step.[72] Moreover, the hemilability of the ligand coordination, such as with N or P groups, allows for the stabilization of actives species and for the coordination of substrates.

In particular, two types of active nickel species were described though the action of activating agent (cocatalyst) in ethylene oligomerization (Fig. 2):

– cationic species, highly electrophilic, isolated by Wilke *et al.* in 1966[73] from neutral ligand;

– neutral species, less electrophilic and isolated by Keim *et al.* in 1978[74] from monoanionic ligand.

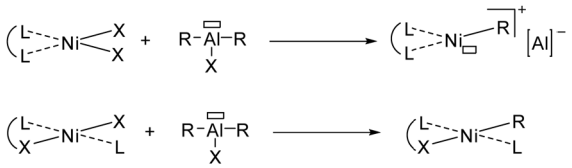

Fig. 2 Neutral ligand to cationic catalyst (top) and anionic ligand to neutral catalyst (bottom) upon activation with Al-based cocatalyst.

Among bidentate neutral ligands, the α-diimine ligands developed by Brookhart[61] allowed for producing highly electrophilic nickel(II) active species upon activation and favoring olefin insertion through β-H elimination (Fig. 2).[75]

In contrast, monoanionic ligands give rise to neutral nickel(II) active species (Fig. 2). Highly productive (P,O)-based nickel(II) catalysts pioneered by Keim, known as SHOP catalysts,[76] and (N,O)-based phenoxyimine analogues by Grubbs[63] were found to produce α-olefins in a broad Schulz–Flory distribution, implying that short oligomers are favored, as well as polyethylene with high molecular weight.

The Shell Higher Olefin Process (SHOP) relies on a nickel-based catalyst with a P–O ligand developed by Keim in 1978 (Fig. 3). This type of catalyst is synthesized with a phosphorus ylide, a [Ni(1,5-cyclooctadiene)$_2$] (Ni(COD)$_2$) complex and a phosphine.[77] SHOP-based catalysts with a phosphino-enolate component favors the elimination step rather than the propagation step, leading to LAOs up to twenty carbon atoms. Removing the phosphine part with a scavenger would lead to a polymerization catalyst rather than an oligomerization catalyst.[74,78–80] The SHOP process enables to produce a broad range of oligomers but mainly C_{12} to C_{20+} olefins and one of the challenge remains to make this type of catalyst more selective towards 1-butene.

3. Molecular Ni catalysts grafted onto siliceous materials

3.1 Purely inorganic supports

In the field of heterogeneous catalysis, inorganic solids are the most established supports, with siliceous-based materials at the forefront. This section will review the state of the art for ethylene oligomerization by this class of materials.

Lallemand *et al.* tested different types of zeolitic materials (Ni-MCM-36 and Ni-MCM-22) for ethylene oligomerization.[81–83] The catalysts are obtained from zeolite structures, by cation exchange. Cations are used during zeolite synthesis in order to ensure charge neutrality within the structure. The pristine materials underwent a treatment with an ammonium nitrate solution in order to replace the cations and then the ammonium ions were replaced by nickel cations. This technique of cation exchange with zeolites (for ethylene oligomerization purposes) enables to obtain an optimal dispersion of the catalytic active sites throughout the support, since they also participate to the structure's charge neutrality and do not require any activation with an aluminum-based cocatalyst. However, the activation of the catalyst requires high temperatures in order to desorb any impurities within the pores and to obtain an optimal porosity for the reaction. The authors postulated that this activation was responsible for the occurrence of acidic sites and the reduction of Ni^{2+} sites into Ni^{+} sites. For a reaction time of 30 minutes, under 40 bar of ethylene at 70 °C, the catalysts Ni-MCM-36 and Ni-MCM-22 respectively achieved 1.1 and 10 $g_{oligomers}\ g_{catalyst}^{-1}\ h^{-1}$ with a selectivity in butene around 81% in both cases. A product distribution close to a Schulz–Flory one is described by the authors and they noticed the higher production of 2-butene, which could be attributed to the acidic sites, decreasing the selectivity in LAOs.

In 2011, with the NiMCM-41 catalyst, the authors observed a Schulz–Flory distribution of the products. This distribution remained steady during seven days at 30 °C and 30 bar of ethylene in continuous flow, with an initial activity of 6.7 $g_{oligomers}\ g_{catalyst}^{-1}\ h^{-1}$. The production of heavier oligomers, due to acidic sites increasing the dimerization of lighter olefins, can lead to micropores blocking (3.5 nm for NiMCM-41) and the high temperatures (150 °C) can boost coke production. These two phenomena, due to a lack of control on the nickel environment, can lead to the deactivation of the catalyst.

More recently, in 2020, Andrei *et al.* reported the use of amorphous $AlSiO_2$ and ordered AlSBA-15, mesoporous aluminum silicates.[84] The Ni–$AlSiO_2$ and Ni–AlSBA-15 were prepared the same way as described previously, by ammonium nitrate treatment and with nickel nitrate hexahydrate. The catalysts were tested for ethylene oligomerization. Despite initial conversion of 87% and 80%, respectively for Ni–AlSBA-15 and Ni–$AlSiO_2$ with selectivities in butene of 55 wt% and 58 wt%, the authors proved by TGA analysis that heavier products (C_8 and higher olefins) were responsible for catalyst deactivation, especially due to acid sites. Ni–$AlSiO_2$ with a wider pore width than Ni–AlSBA-15 underwent a less significant deactivation.

The Ni exchange technique does not allow control over the active site's environment. The exact nature of the active sites is still unknown and the occurring mechanism is not fully understood.[50] Acid sites represent also another type of active sites, responsible not only for isomerization reactions but also for dimerization of the products formed in the first place. Combined to the microporosity of some catalysts, the production of heavier products (C_8 and more) can lead to pore blocking. Working at higher temperatures also favors catalytic cracking of the products.

Surface organometallic chemistry has been used for the synthesis of two mesoporous silica-grafted catalysts for ethylene oligomerization:

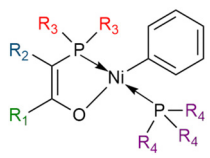

Fig. 3 SHOP catalyst with different groups that enable to tune its activity and selectivity (R = alkyl or aryl).

– a tantalum-based catalyst, [(≡SiO)$Ta^{V}Cl_2Me_2$], by grafting $TaMe_3Cl_2$ on SBA-15[85]

– a niobium-based catalyst, [(≡SiO)$NbMe_4$], resulting from the grafting and methylation of $NbMe_2Cl_3$ on a SiO_2 surface dehydroxylated at 700 °C.[86]

The niobium-based catalyst enabled to achieve 91.9 wt% of butene selectivity with an activity of 1050 $mol_{ethylene\ consumed}$ mol_{Nb}^{-1} h^{-1} under 50 bars of ethylene at 100 °C during one hour in toluene. In similar conditions (30 minutes of reaction instead of one hour), the tantalum-based catalyst's activity reached 375 $mol_{ethylene\ consumed}$ mol_{Ta}^{-1} h^{-1} with 82.7 wt% of hexene products. Both catalysts are active without aluminum-based cocatalyst activation. However, they suffered from deactivation by polyethylene production, stemming from the complexes geometry and coordination sphere on the surface.[87] Hence, the interactions between the active sites and the free oxide or hydroxide sites might hamper the catalytic activity.[6,20,88,89]

3.2 Hybrid periodic mesoporous silica

Periodic Mesoporous Organosilica (PMOs) is a class of siliceous materials with organized mesoporosity and possibly containing organic moieties.[20,90,91] They present high surface areas, high porous volume and structural diversity (MCM-48 with a 3D porous structure or MCM-50 with a 2D structure). Aluminum can be introduced into the structure to tune its acidity.

Recently, Shin *et al.* synthesized a series of eight bpy-SBA-15, with different molar amounts of bipyridyl (bpy) sites metalated with $NiCl_2{\cdot}H_2O$ (Fig. 4).[92] The design of these catalysts was motivated by the attempt to minimizing polyethylene formation and improving oligomer production, with heterogeneous (bpy)Ni(II)Cl_2 catalysts.

Ethylene oligomerization was performed in heptane during 30 minutes with 70 or 700 equivalents of Et_2AlCl compared to Ni and under 30 bar of ethylene, at 150 °C. First, the series of catalysts were more active than their homogeneous counterpart Ni(bpy)Cl_2 for the given conditions, with 406 $mol_{oligomers}$ mol_{Ni}^{-1} h^{-1} and a selectivity in butene of 51%. The authors observed minimal polyethylene formation with the catalyst made with 0.21 wt% of Ni and a 4 nm pore size. It achieved 4422 $mol_{oligomers}$ mol_{Ni}^{-1} h^{-1} and a selectivity in butene of 77%, with 700 equivalents of Et_2AlCl. The catalyst has been recycled seven times, without nickel leaching, suggesting the successful immobilization of the molecular complex within the large pores of the material. However, catalysts with higher pore sizes (7 and 10 nm) and higher nickel loadings (0.27 wt% and 0.31 wt% of Ni respectively), proved to be less active and less butene-selective in the same conditions. Same conclusions can be drawn for 2.25 wt% and 1.51 wt% nickel loadings.

Different inorganic and non-porous materials have been also synthesized and tested for catalytic purposes, like clays, aluminum sulfates and oxide surfaces, but they will not be developed here since they have not shown particular activity in ethylene oligomerization.[81,93–95]

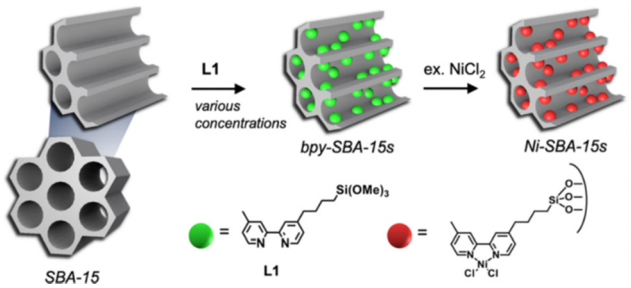

Fig. 4 From a synthesized SBA-15 PMO, the design of a series of eight bpy-SBA-15 (bipyridyl sites embedded on the surface and within the walls of the structure) and their metalation with $NiCl_2{\cdot}H_2O$. Reprinted from *Appl. Catal., A*, **590**, Shin *et al.*, A Way to Avoid Polymeric Side Products during the Liquid-Phase Ethylene Oligomerization with SBA-15 Supported (Bpy)Ni(II)Cl_2 Heterogeneous Catalyst, p. 117363, Copyright (2020), with permission from Elsevier.[92]

4. Molecular Ni catalysts embedded into porous polymeric materials

In contrast to siliceous materials, molecular complexes heterogenized within porous polymers can be embedded within the porous network, with a high site density per volume and per mass of solid. Moreover, the high porosity of the solids allows for high accessibility of the active sites. Porous polymers of hybrid organic–inorganic nature like Metal–Organic Frameworks (MOF),[96–104] or purely organic, like Porous Organic Polymers (POP) or Porous Organic Networks (PON) can be made by design using coordinating motif as organic repeating unit.[105–113] MOF and POP both allow for a wide versatility in composition and porous network topology by varying organic linkers/monomers (for MOF and POP) and metal nodes (in MOF). The crystalline MOF present well-defined topologies and their extended ordered nature allows for the control over grafted sites environment within the MOF pores and in-depth mechanistic studies using computational chemistry (Fig. 5).[114–117] In contrast, POP/PON are amorphous or semi-crystalline and present a more disordered network which however is made by C–C bonds, much more stable than the MOF coordination bonding towards hydrolysis, for example.[118] Among porous organic

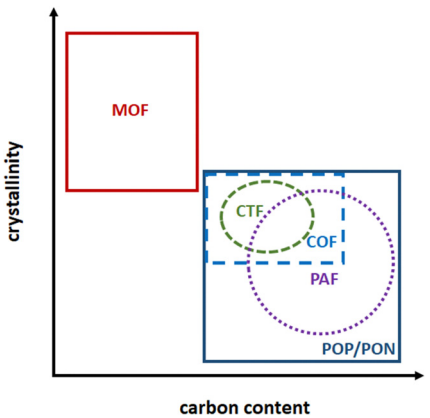

Fig. 5 Representation of classification of non-siliceous polymeric porous materials. (MOF: metal–organic frameworks; POP: porous organic polymers; PAF: porous aromatic frameworks; PON: porous organic networks; COF: covalent organic frameworks; CTF: covalent triazine frameworks).

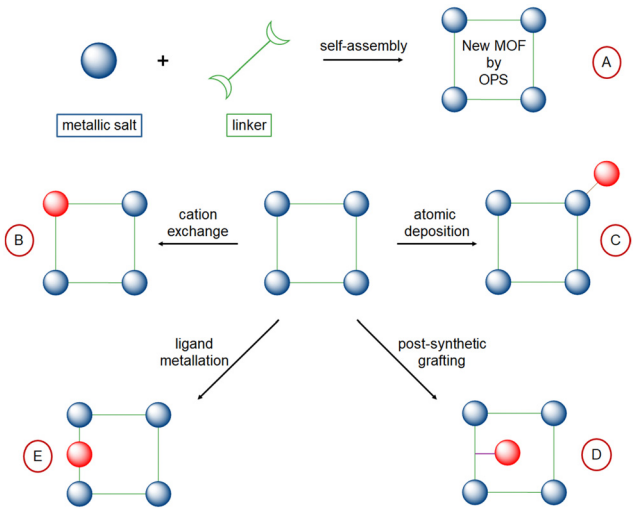

Fig. 6 Different synthetic pathways to get isolated active sites within MOF.

polymers, Porous Aromatic Frameworks (PAF) are rigid frameworks where C–C bonds connect aromatic units,[119] Covalent Organic Frameworks (COF) are slightly crystalline layered materials[120,121] and covalent triazine frameworks (CTF) are a sub-class of COF having triazine units as node (Fig. 5).[122–124]

Different methods have been employed to embed isolated active sites for ethylene oligomerization within MOF and POP porous frameworks (Fig. 6):

– by one-pot synthesis, with Ni active sites already incorporated within the structure of the MOF (route A);[125]

– by cation exchange in the MOF inorganic node (route B);[126,127]

– by atomic deposition onto the MOF inorganic node (route C);[32,33]

– by post-synthetic grafting of pending ligand inside the MOF (route D);[128–130]

– by coordination of metal cation into porous structures containing vacant coordination sites as building monomers, *i.e.* bipyridine[131–134] or phenoxy-imine (route E).[135]

4.1 Self-assembled Ni-based MOF (route A)

In the following examples, the MOF are synthesized using nickel salt through one-pot synthesis (OPS). The nickel is thus present either coordinated to oxygens from carboxylates or to nitrogen from imidazolates, either as single atom or as a dimer within a paddle-wheel complex.

Ni-carboxylate MOF. In 2018, Hu *et al.* developed nickel-based MOF nanosheets (Ni-UMOFNs), based on benzene-1,4-dicarboxylate.[136] This MOF synthesis pathway enables to obtain nickel-based stacked sheets, with isolated and full-exposed active sites. Prior to catalytic experiments, Ni-UMOFN was activated under vacuum at 190 °C, hence achieving Ni-UMOFN-190. Ethylene oligomerization experiments were performed in toluene at 25 °C and 10 bars of ethylene. Catalysts were activated with 500 equivalents of Et_2AlCl and achieved, after one hour of reaction, a TOF of 5536 $mol_{ethylene\,consumed}$ mol_{Ni}^{-1} h^{-1} with a selectivity in butene of 75.6%. With the same catalyst, a TOF of 3000 $mol_{ethylene\,consumed}$ mol_{Ni}^{-1} h^{-1} was already achieved after thirty minutes of reaction with a selectivity in butene of 76.6% whereas a lower TOF of 2500 $mol_{ethylene\,consumed}$ mol_{Ni}^{-1} h^{-1} could be observed after one hour and a half, with an improved selectivity in butene of 90.2%. Atomic Force Microscopy (AFM) analysis enabled the authors to evaluate the thickness of the catalyst nanosheets after four recycling experiments. For one hour of reaction, Ni-UMOFN-190 achieved 4893 $mol_{ethylene\,consumed}$ mol_{Ni}^{-1} h^{-1} with a 72.1% butene selectivity for a first cycle compared to 3929 $mol_{ethylene\,consumed}$ mol_{Ni}^{-1} h^{-1} with a 71.4% butene selectivity for a fourth cycle. The stable catalyst activity was attributed to the fact that fresh nickel active sites are continuously exposed to aluminum-based cocatalyst and ethylene.

Later, in 2019, Kaskel and coworkers proposed seven nickel-based MOFs, synthesized by one-pot synthesis for ethylene oligomerization (Fig. 7):[137] the CPO-27(Ni) or $[Ni_2(dhtp)]_n$ from a mixture of a nickel(II) acetate tetrahydrate in 1-butanol with 2,5-dihydroxyterephtalic acid ($dhtpH_2$), the $[Ni(bdc)(dabco)]_n$ and $[Ni(bdc)(dabco)_{0.5}]_n$ (bdc = 1,4-benzenedicarboxylate and dabco = 1,4-diazabicyclo[2.2.2]octane, and the $[Ni_3(ndc)_3(DMF)_2((CH_3)_2NH)_2]_n$ (ndc = 2,6-naphtalenedicarboxylate and DMF = *N*,*N*-dimethylformamide). The DUT-8(Ni) or $[Ni(ndc)(dabco)_{0.5}]_n$ was obtained, from a mixture of nickel(II) nitrate hexahydrate in DMF with 2,6-naphtalenedicarboxylic acid and dabco, in two forms, $[Ni(ndc)(dabco)_{0.5}]_n$_rigid and $[Ni(ndc)(dabco)_{0.5}]_n$_flexible. The two forms differ by the fact that the flexible DUT-8(Ni) can switch between open and close pore form whereas rigid DUT-8(Ni) remains in the open pore. Each nickel-node represents an isolated active site for ethylene oligomerization. Prior to ethylene oligomerization experiments, the authors evaluated the integrity of the Ni-based MOFs after leaving them to stir overnight with Et_2AlCl (Al/Ni = 17) in toluene. Powder X-ray diffraction (PXRD) measurements showed that only CPO-27(Ni), $[Ni_3(ndc)_3(DMF)_2((CH_3)_2NH)_2]_n$, DUT-8(Ni)_rigid and DUT-8(Ni)_flexible remained structurally unchanged, compared to the other MOFs.

The authors tested these seven catalysts for ethylene oligomerization in toluene, activated with 17 equivalents of Et_2AlCl at 21 °C and 10 bars of continuous ethylene feed. The catalytic activities ranged from 1 $mol_{oligomers}$ mol_{Ni}^{-1} h^{-1} (100% C_4 selectivity) with the CPO-27(Ni) to 49 $mol_{oligomers}$ mol_{Ni}^{-1} h^{-1} with $[Ni_3(ndc)_3(DMF)_2((CH_3)_2NH)_2]_n$ (50% selectivity in C_4) and DUT-128 (47% selectivity in C_4). It is noteworthy that with these nickel-based MOFs no polymeric product could be observed.

More recently, another nickel carboxylate MOF, Ni-MIL-77,[139] has been synthesized by Wang and coworkers, using glutaric acid as linker. This MOF can present distinct 1D or 3D topology as confirmed by PXRD, however without a clear evidence of porosity.[140] Under 10–20 bars pressure range of ethylene and using between 80 to 210 equivalent of Al-based cocatalyst, the 1D Ni-MIL-77 was found to perform the best with a TOF of 5544 h^{-1} and a selectivity of 98% for butenes. Unfortunately, the solid catalysts showed a drastic loss of crystallinity after reaction and could not be efficiently reused. Indeed, the authors found that hydrolysis products from the Al-

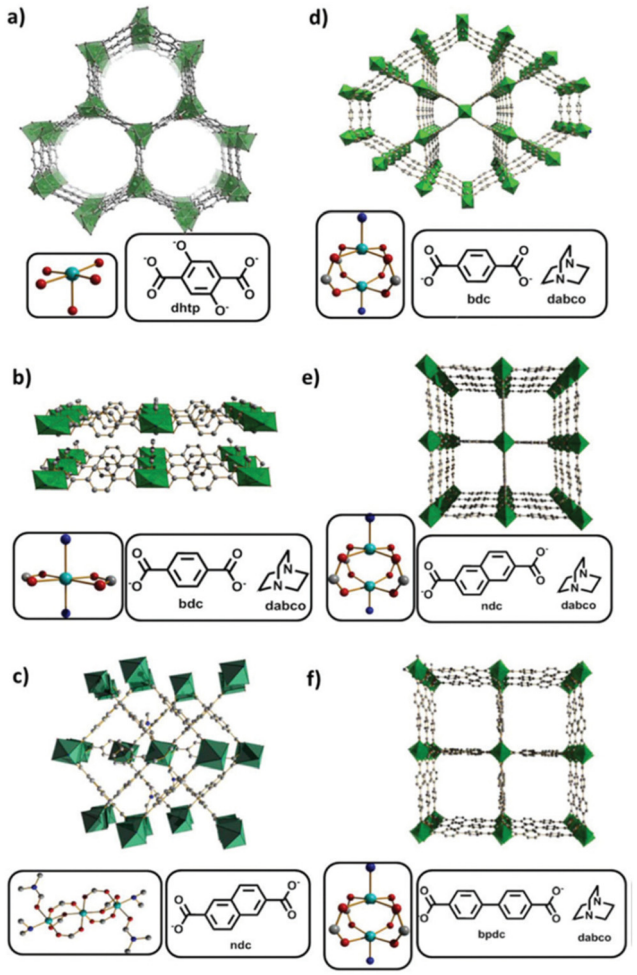

Fig. 7 (a) CPO-27(Ni); (b) $[Ni(bdc)(dabco)]_n$; (c) $[Ni_3(ndc)_3(DMF)_2((CH_3)_2NH)_2]_n$; (d) $[Ni(bdc)(dabco)_{0.5}]_n$; (e) DUT-8(Ni); (f) DUT-128. Reproduced from ref. 138 with permission from the Royal Society of Chemistry.

based cocatalyst cover the MOF's surface leading to catalyst deactivation.

Ni-imidazolate MOF. In 2021, Chen *et al.* proposed the one-pot synthesis of a Ni-ZIF-8 MOF for the selective dimerization of ethylene.[125] From a mixture of $Zn(NO_3)_2{\cdot}6H_2O$ and $Ni(NO_3)_2{\cdot}6H_2O$ with 2-methylimidazole as linker, the authors synthesized four different Ni-ZIF-8 MOFs by varying the molar amount of the Zn and the Ni salts, in order to achieve different nickel loadings from 0.08 to 0.70 wt%. They speculated that the active Ni^{2+} imine-like site, remains at the surface of the crystals, and not within the porosity of the material, which enables to circumvent mass-transport limitations within the porosity of the material (Fig. 8). The authors also prepared another catalyst by growing a ZIF-8 shell on the Ni-ZIF-8 surface, namely Ni-ZIF-8@ZIF-8, in order to cover-up the surface nickel active sites and observe its catalytic activity. The ethylene oligomerization experiments were performed in toluene during ten minutes, the catalysts being activated with methylaluminoxane (MAO, between 660 and 19 900 equivalents), under 30 bars of ethylene and at 35 °C.

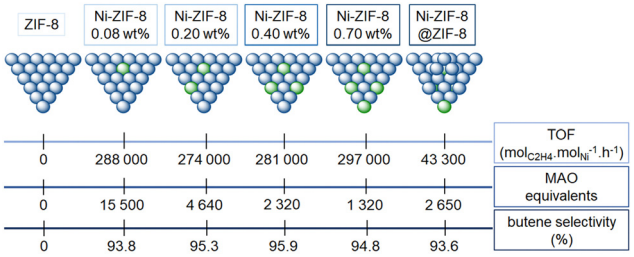

Fig. 8 Representation of the ethylene oligomerization TOF (top), of the MAO equivalents used (in toluene, at 35 °C and 30 bar of ethylene; middle) and of the butene selectivity (bottom) with ZIF-8, four different catalysts obtained from ZIF-8 and exhibiting different nickel loadings (0.08, 0.20, 0.40 and 0.70 wt%) and Ni-ZIF-8@ZIF-8.[125]

First, the ZIF-8 itself (with only Zn sites) was not active whereas all the other Ni-ZIF-8 catalysts generate oligomers (whatever the loading or the catalytic conditions), indicating the necessity of nickel sites in order to observe a catalytic activity. Besides, for given conditions, the Ni-ZIF-8 was seven times more active than the Ni-ZIF-8@ZIF-8, indicating that only some of the nickel active sites on the surface have been deactivated by the ZIF-8 growth. No polyethylene was reported by any Ni-ZIF-8 catalyst, with butene selectivities above 90%. Among nickel-based catalyst discussed so far, Ni-ZIF-8 catalyst seems to be more active and selective towards butene than other self-assembled nickel-based MOF catalysts, for the given conditions in each work. The catalytic activity enhancement of the Ni-ZIF-8 catalyst could stem from the fact that the macroligand is made of imine-like moieties. The effects of the thousand-fold excess of alkyl aluminum seems poorly understood (from 1320 to 15 500 equivalents to Ni, see Fig. 8).

As an alternative to ZIF-8, Dong and coworkers recently reported Ni-ZIF-L as highly active ethylene dimerization catalyst.[141] ZIF-L present similar composition and chemical environment than ZIF-8 but with different topology, with quite lower surface area of *ca.* 160 $m^2\ g^{-1}$, which allows the insertion of nickel atoms only at the surface of the MOF's particles. According to the authors, the 2D leaf-like shape of ZIF-L would allow for higher external accessible surface compared to ZIF-8. Using MAO as cocatalyst under 30 bars of ethylene and 30 °C in toluene, the NI-ZIF-L allowed accessing ethylene dimerization with a TOF of 330 230 h^{-1} with a selectivity in 1-butene higher than 90%. Unfortunately, after one hour of reaction, the measured selectivity in 1-butene slightly dropped from 95% to 77% (overall C4 selectivity constant from 97% to 94% with same TOF), likely due to butene isomerization by Lewis acid sites either from the MOF or the cocatalyst, and the possible recycling of the catalyst was not demonstrated.

4.2 Single sites by Ni cation exchange in MOF (route B)

Following the above-described examples of Ni-based MOF, nickel sites can be introduced post-synthetically by replacing metal cations natively present at the MOF node, thus generating isolated active sites for ethylene oligomerization.

MFU-4. In 2016, Dincă and coworkers reported the cation-exchange of the Zn^{2+} ions by Ni^{2+} ions of the MFU-4*l* MOF

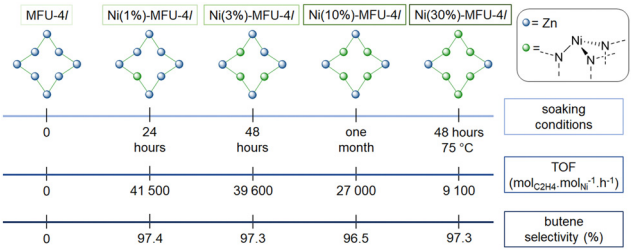

Fig. 9 Representation of the effect of soaking conditions for MFU-4*l* in a $Ni(NO_3)_2{\cdot}6H_2O$ DMF solution on the number of Zn^{2+} replaced by Ni^{2+} (top), of the nickel loading on the ethylene oligomerization TOF (led in toluene, at 25 °C and 50 bars of ethylene and activated with 500 equivalents of MAO) (middle) and on the butene selectivity (bottom).

($Zn_5Cl_4(BTDD)_3$, with H_2BTDD for bis(1*H*-1,2,3-triazolo[4,5-*b*],[4′,5′-*i*])dibenzo[1,4]dioxin).[127] An MFU-4*l* is soaked in a DMF solution of $Ni(NO_3)_2{\cdot}6H_2O$. The longer the pristine material is left to soak, the higher Zn^{2+} replace by Ni^{2+}. This method resulted in the synthesis of three additional catalysts: Ni(10%)-MFU-4*l*, Ni(3%)-MFU-4*l* and Ni(1%)-MFU-4*l* (Fig. 9).

Ni-CFA-1. Later, in 2019, the same group developed a Ni-CFA-1 MOF, formulated as $Ni_5(OAc)_4(bibtz)_3$ (H_2bibtz = 1*H*,1′*H*-5,5′-bibenzo[*d*][1,2,3]triazole), isoreticular to and more scalable than analogous Ni-MFU-4*l* based on costly bis(1H-1,2,3-triazolo-[4,5-*b*],[4′,5′-*i*])dibenzo[1,4]dioxin ligand.[142] Two Ni-CFA-1 catalysts were synthesized by varying nickel content, Ni(7.5%)-CFA-1 and Ni(1%)-CFA-1. They were prepared according to the same procedure as Ni-MFU-4*l*. CFA-1 structure enabled to keep the imine-like coordination, observed with MFU-4*l*, towards isolated nickel active site (Fig. 10).

Ethylene oligomerization was performed in toluene with 50 to 2000 equivalents of MMAO-12, under 50 b of ethylene at 22 °C. Under similar conditions, Ni(1%)-CFA-1 achieved 1800 $mol_{ethylene\ converted}\ mol_{Ni}^{-1}\ h^{-1}$ with a 88.6% butene selectivity whereas Ni(1%)-MFU-4*l* enabled to achieve 41 500 $mol_{ethylene\ converted}\ mol_{Ni}^{-1}\ h^{-1}$, with a 97.4% butene selectivity when activated with 500 equivalents of MAO.

4.3 Single sites by atomic Ni deposition on MOF (route C)

So far, this methodology relies on the use of zirconium oxo clusters of Zr-based MOF as a model inorganic surface to graft nickel precursors.

Ni-AIM-NU-1000. Based on previous research work performed on atomic deposition on MOF (AIM), Farha and coworkers established a method to deposit isolated Ni ions on the Zr nodes of the NU-1000, a highly robust MOF made with Zr_6 oxo clusters linked by 1,3,6,8-tetrakis(*p*-benzoate)pyrene.[32] Upon activation with Et_2AlCl, the authors tested the Ni-AIM-NU-1000 for gas-phase ethylene oligomerization at 45 °C and 2 bar pressure in a continuous reactor. Polymeric product was formed during the first 10 hours of the process and afterwards oligomers could be observed with a butene selectivity around 42% with a TOF of 1080 h^{-1}. The findings on catalytic behavior of the heterogenized Ni sites were supported by computational data at the DFT level. By using the same strategy, a Co-AIM-NU-1000 was developed and its activity appeared to be lower than Ni-AIM-NU-1000.[33] In a later work, the same group tuned the electronic and steric environment of the active site of the Ni-AIM-NU-1000 with the electron-withdrawing group hexafluoroacetylacetonate (Facac) and the weakly electron-donating group acetylacetonate (Acac). They evaluated the effects of this tuning with the catalytic ethylene oligomerization, in a packed reactor under continuous flow of 100% ethylene gas feed at 2 bar and 45 °C, activated with Et_2AlCl.[143] Despite a twenty-fold lower activity of these materials compared to Ni-Facac-AIM-NU-1000, the two electronically/sterically tuned catalysts afforded 100% selectivity in butene (Fig. 11). A Gibbs free energy profile, with a model where the Zr_6 node is functionalized with both a single Ni atom and a Facac or Acac ligand, enabled to show that with these specific ligands, the butene production is energetically more favorable than chain growth. However, since the comparison of selectivity has been made at different conversions, unambiguous conclusions can be hardly raised from these data.

Ni/UiO-66. More recently, Bhan, Gagliardi and coworkers followed the same methodology to study nickel-functionalized UiO-66.[144] Such as in NU-1000 described above, the UiO-66 MOF contains zirconium-based inorganic node in which nickel atoms can be deposited at defective sites, typically in place of missing linkers. The catalytic behavior of Ni/UiO-66 catalyst has been studied under gas phase conditions without any external cocatalyst. After a pressure-dependent induction period, the catalyst showed a stable oligomerization rates for more 15 days on ethylene stream. Using *in situ* NO titration, the authors demonstrate that the number of active Ni sites increased with the ethylene pressure, accounting only for 12% of the nickel

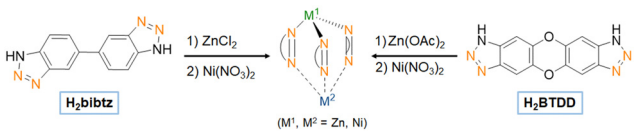

Fig. 10 Representation of how the H_2bibtz (1*H*,1′*H*-5,5′-bibenzo[*d*][1,2,3]triazole)) linker and the H_2BTDD linker, used respectively to synthesize CFA-1 and MFU-4*l* enable to obtain the same scorpionate-like configuration with three coordinating nitrogen atoms embedded within the MOF structure.

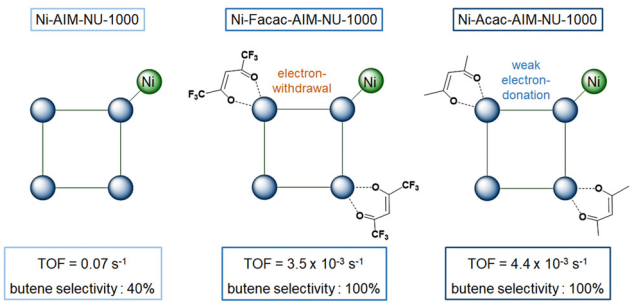

Fig. 11 Ethylene oligomerization catalytic activity obtained with Ni-AIM-NU-1000, Ni-Facac-AIM-NU-1000 and Ni-Acac-AIM-NU-1000 in a packed reactor under continuous flow of 100% ethylene gas feed at 2 bar and 45 °C, activated with Et_2AlCl.

atoms at 1800 kPa, and that ethylene oligomerization was first order in ethylene pressure with an activation energy of 81 kJ mol^{-1} at temperatures from 443–503 K. DFT-level computations using a cluster model of Ni/UiO-66 confirmed the postulated the Cossee–Arlman mechanism.

4.4 Post-synthetic grafting of molecular Ni complexes within MOFs (route D)

In this section, defined nickel molecular complexes are introduced stepwise within the MOF cavity by immobilizing vacant coordinating ligands which are then metallated with a nickel salt.

Ni@(Fe)-MIL-101. Canivet *et al.* achieved the isolation of active sites by the imine condensation of a $Ni(PyCHO)Cl_2$ complex on the dangling amino groups of the (Fe)-MIL-101-NH_2 framework,[91,145] to yield 10Ni@(Fe)-MIL-101 and 30Ni@(Fe)-MIL-101 catalysts, where respectively 10% and 30% of the amino groups were converted into the corresponding nickel imino complex.[78] These two catalysts were tested for ethylene oligomerization in *n*-heptane, with 15 bars of ethylene at 10 °C during one hour and with 70 equivalents of Et_2AlCl per nickel. 10Ni@(Fe)-MIL-101 and 30Ni@(Fe)-MIL-101 achieved a similar catalytic activity (respectively 3166 and 3215 $mol_{oligomers\,formed}$ mol_{Ni}^{-1} h^{-1}, with a selectivity in 1-butene around 94% in both cases), proving that the catalytic sites are accessible (Fig. 12). It can also be assumed that, up to a certain nickel loading, the reaction is not limited by diffusion. It is noteworthy that no catalytic activity could be observed with only (Fe)-MIL-101-NH_2 or with (Fe)-MIL-101-NH_2 put into solution with either $NiCl_2$ or PyCHO and with the filtrated catalytic solution (leaching experiment) re-activated with Et_2AlCl. Catalytic activities of 10Ni@(Fe)-MIL-101 and 30Ni@(Fe)-MIL-101 originate from the nickel-isolated active sites within the framework. In this study, the most competitive result was obtained under mild conditions (25 °C and 30 bar of ethylene, with 70 equivalents of Et_2AlCl) to reach 10 455 $mol_{oligomers}$ mol_{Ni}^{-1} h^{-1} with a 1-butene selectivity above 90%.

IRMOF-3 and MixMOF. Later, in 2014, Liu *et al.* also synthesized a series of NH_2-based MOF from $Zn(NO_3)_2{\cdot}6H_2O$ and aminoterephtalic acid (IRMOF-3) and three MixMOFs (MixMOF-a, MixMOF-b and MixMOF-c), synthesized following the same procedure as IRMOF-3 with aminoterephtalic acid partially substituted with terephtalic acid.[129] The MOFs were post-synthetically modified by imine condensation using $Ni(PyCHO)Br_2$ complex by the same molecular complex immobilization technique as Canivet *et al.*[128] Upon metalation, the authors tested the different catalysts for ethylene oligomerization in toluene, under 20 bar of ethylene, at 20 °C during 30 minutes and activated with 100 equivalents of Et_2AlCl. MixMOFs-Ni-b exhibited a catalytic activity of 6.91×10^4 $g_{oligomers}$ mol_{Ni}^{-1} h^{-1} with a selectivity in butene of 79.5% whereas IRMOF-3-Ni-a achieved a catalytic activity of 6.29×10^4 $g_{oligomers}$ mol_{Ni}^{-1} $h^{-1}$with a butene selectivity of only 35% (Table 1). Comparing IRMOF-3 and MixMOF catalysts, it can be concluded that higher amino content can hamper the catalytic activity and that site dilution might improve diffusion within the pores and thus the catalytic productivity and selectivity.

MIL-125(Ti)-NH_2. Following a similar strategy, Chen *et al.* reported in 2020 the stepwise post-synthetic grafting 2-pyridinecarboxaldehyde in MIL-125(Ti)-NH_2, metallated afterwards with $NiCl_2{\cdot}6H_2O$.[130] Ethylene oligomerization was performed in cyclohexane, with 800 equivalents of MAO at 50 °C and under 10 bar of ethylene during 30 minutes. This catalyst achieved a catalytic activity of 18×10^4 $g_{oligomers}$ mol_{Ni}^{-1} h^{-1} with a butene selectivity of 19.6 wt%, corresponding to 27% in moles of products formed, and including 87.2 wt% of 1-butene.

NU-1000. Farha and coworkers used as a platform the NU-1000 MOF, with a molecular formula $Zr_6(\mu^3\text{-}OH)_8(OH)_8(TBAPy)_2$ (H_4TBAPy being 1,3,6,8-tetrakis(*p*-benzoic acid)pyrene) to perform condensation of phosphonate-functionalized bipyridyl coordinating sites on the Zr node of the MOF, dangling bipyridine being then metalated with a $NiCl_2$ salt.[146] The catalytic tests were performed afterwards in heptane, at 21 °C under 15 bar of ethylene, the catalyst being activated with 70 equivalents of Et_2AlCl during one hour. NU-1000-bpy-$NiCl_2$ allowed to achieve an intrinsic catalytic activity for butenes of 1950 h^{-1}, with a selectivity in butene of 93%. The same catalyst showed similar activity for gas-phase reaction.

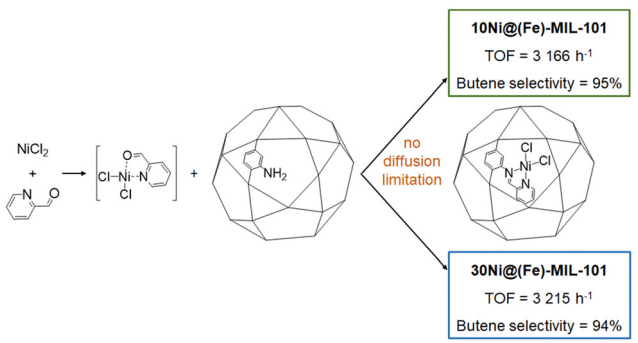

Fig. 12 10Ni@(Fe)-MIL-101 and 30Ni@(Fe)-MIL-101 catalytic activity under 15 bars of ethylene at 10 °C with 70 equivalents of Et_2AlCl per nickel.

4.5 Nickelation of MOFs and POPs macroligands (route E)

In contrast to the previously described methods, here the MOFs and POPs are not used as support to graft molecular complex at the pore surface but are envisioned as porous macroligands, *i.e.* solids acting as the organic ligand in the molecular complex. The MOFs and POPs described below are made using coordinating linkers/monomers which are derivatized from known efficient organic ligands in molecular complexes.

[Al/Ni]–Ni-bpydc MOFs. Kyogoku *et al.* initiated the research in 2010 with two MOFs: [Al]–Ni-bpydc (MOF) and [Ni]–Ni-bpydc (MOF).[133] They were respectively synthesized by One-Pot Synthesis of $Al(NO_3)_3{\cdot}9H_2O$ with a Ni-bipyridyl-dicarboxylic acid in DMF and of $Ni(NO_3)_2{\cdot}6H_2O$ with bipyridyl-dicarboxylic acid. Ethylene oligomerization catalytic tests were conducted in heptane, at 5 °C during one hour, under 15 bar of ethylene, the catalyst being activated with 70 equivalents of Et_2AlCl. [Al]–Ni-bpydc (MOF) and [Ni]–Ni-bpydc (MOF) both exhibited a productivity of *ca.* 20 $g_{oligomers}$ $g_{catalyst}^{-1}$ h^{-1} and a 13% conversion, with selectivities in butene of 89.1% and 92.7%, respectively.

Table 1 Characteristics and catalytic activity comparison between Ni-loaded iminopyridine-functionalized MOF catalysts for ethylene oligomerization. Data are directly extracted or calculated from the corresponding published reports

MOF catalyst	NH_2 content[a] (10^{-4}mol g^{-1})	surface area before PSM[b] (m^2 g^{-1})	surface area after PSM[b] (m^2 g^{-1})	Ni content[c] (10^{-3}mol g^{-1})	catalytic activity (10^4 $g_{oligomers}$ mol_{Ni}^{-1} h^{-1})	Butene selectivity (%)	Ref.
MixMOFs-Ni-a	5.95	1080	262	0.65	5.8	71.3	129
MixMOFs-Ni-b	8.12	1213	176	1.07	6.9	79.5	129
MixMOFs-Ni-c	10.95	1671	125	1.22	5.6	79.5	129
IRMOF-3-Ni-a	36.81	1086	8	0.17	6.3	35	129
30Ni@(Fe)MIL-101	42.86	1884	155	1.12	58.5	94	128
Ni@(Ti)MIL-125-NH_2	36.29	1164	1083	0.23	18.0	27	130

[a] As determined by elemental analysis. [b] As determined from nitrogen physisorption isotherm using BET method. [c] As determined by ICP analysis.

Zr-MOFs. Later, in 2017, Long and coworkers proved that site dilution within a porous framework enables to improve diffusion of the reagents and the substrates towards the active sites and of the products off the porous framework. The authors synthesized a UiO-67, made only with biphenyl-4,4′-dicarboxylate (bpdc), and two UiO-67-bpy frameworks made using additional 2,2′-bipyridine-5,5′-dicarboxylate (bpydc) with different amounts of bipyridyl sites, with the respective formula $Zr_6O_4(OH)_4(bpydc)_{0.84}(bpdc)_{5.16}$ and this $Zr_6O_4(OH)_4(bpydc)_{0.84}(bpdc)_{5.16}$, to be compared with UiO-67-bpy, formulated as $Zr_6O_4(OH)_4(bpydc)_6$, that only contains bipyridyl sites (Fig. 13).[131] Each material was post-synthetically metallated with $Ni(DME)Br_2$ (DME for dimethoxyethane), using 1.0 equivalent of Ni per bpy site and ICP-OES analysis enables to confirm that all the bipyridine sites of the UiO-67-bpy materials were coordinated by $NiBr_2$. More surprisingly, the UiO-67 material, containing no bipyridyl coordinating sites, turned to contain 2.3% Ni for each Zr center (obtained by ICP-OES, which would represent 0.06 wt% of Ni for this catalyst), despite several washings with dimethoxyethane in order to remove any physisorbed Ni complex. Authors assumed that Ni got coordinated to water and hydroxyl ligands on zirconium nodes. The three catalysts were evaluated for ethylene oligomerization in cyclohexane, with 59 bars of ethylene at 55 °C during one hour and with 100 equivalents of Et_2AlCl per nickel. The authors observed a slightly higher activity using $Zr_6O_4(OH)_4(bpydc)_{0.84}(bpdc)_{5.16}(NiBr_2)_{0.84}$ with a productivity of 370 $g_{product}$ $g_{catalyst}^{-1}$ h^{-1}, than with $Zr_6O_4(OH)_4(bpydc)_6(NiBr_2)_6$ with a productivity of 220 $g_{product}$ $g_{catalyst}^{-1}$ h^{-1} (Fig. 13). Along with oligomers, polyethylene was also formed with the $Zr_6O_4(OH)_4(bpydc)_6(NiBr_2)_6$ catalyst.

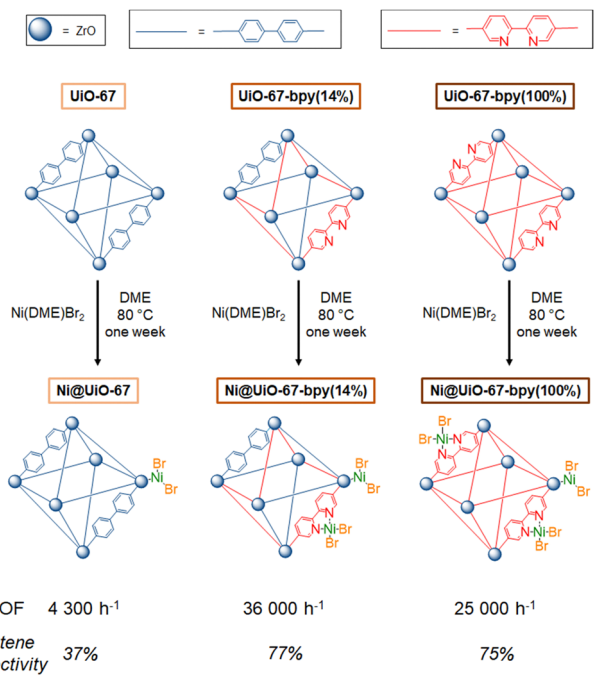

Fig. 13 Metalation procedure of UiO-67, UiO-67(bpy14%) and UiO-67(bpy100%) with $Ni(DME)Br_2$ and TOFs and selectivity under the following conditions: 59 bars of ethylene at 55 °C during one hour and with 100 equivalents of Et_2AlCl per nickel.

These results showed that, in this case, higher metal loadings might lead to detrimental steric hindrance around the active sites consequently leading to polyethylene production. Furthermore, the authors cannot rule out a catalytic contribution from wild nickel sites at the MOF node with nevertheless a negligible impact on the overall productivity and selectivity.

In 2020, Kaskel and coworkers synthesized two imine-based MOFs, PCN-161 and PCN-164, and one phenoxy-imine novel MOF, DUT133.[135] For PCN-161 and PCN-164, the imine condensation between 4-formylbenzoic acid and 4-aminobenzoic acid and *p*-phenylenediamine, respectively, in presence of $ZrCl_4$, enables to achieve imine-based MOFs. The authors also proposed the DUT-133 framework, isoreticular to PCN-161, where the imine condensation of 4-formyl-3-hydroxybenzoic acid with 4-aminobenzoic acid, in presence of $ZrCl_4$, enables to achieve a phenoxy-imine based MOF. The nitrogen physisorption measurements highlighted the microporosity of the material, making it suitable for the immobilization of a molecular complex within its structure. After metallation with $NiCl_2$, ethylene oligomerization has been carried out in an autoclave with 1,2-dichlorobenzene and 51 equivalents of Et_2AlCl at 21 °C and under 15 bars of ethylene. The authors also synthesized a $NiCl_2$@UiO-67(bpydc) catalyst, similar to the one developed by Long and coworkers.[131] The authors compared the 63%NiCl@DUT-133 (63% Ni loading verified by ICP-OES) to $NiCl_2$@UiO-67(bpydc) (with a 5.3% Ni loading verified by ICP-OES) under the same catalytic conditions described before. $NiCl_2$@UiO-67(bpydc) proved to be two times more active and less butene-selective (25 $mol_{oligomers}$ mol_{Ni}^{-1} h^{-1} with 28% of butene) than 63%NiCl@DUT-133 (12 $mol_{oligomers}$ mol_{Ni}^{-1} h^{-1} with 100% butene). It could be concluded that, within Zr-MOF, a Ni active site coordinated to a

phenoxy-imine would be less active and more selective towards butenes than a Ni complex coordinated to a bipyridyl site. The phenoxy-imine seems to favor β-H elimination over propagation step whereas the bipyridyl one favors propagation step, for the given catalytic conditions.

POP-1. In 2017, Kim *et al.* proposed for the first time the immobilization of a nickel complex within a bipyridyl-based porous organic polymer (POP), used for ethylene oligomerization.[132] The pristine material, named as POP-1, was obtained by reaction between tetra(4-azidophenyl)methane and 5,5′-diethynyl-2,2′-bipyridine tectons. Nitrogen physisorption measurement highlighted the microporosity of POP-1 and its suitability to immobilize a molecular complex within its structure. TGA analysis showed the thermal stability of the support up to 300 °C. Metalation was done afterwards by placing the bpy-based POP-1 in a mixture of $NiCl_2{\cdot}H_2O$ dissolved in DMF, in order to get the Ni(II)-POP-1 catalyst. Ethylene oligomerization experiments were performed in heptane, with 70 equivalents of Et_2AlCl compared to Ni during one hour, at 20 °C and under 20 bar of ethylene. Ni(II)-POP-1 achieved a catalytic activity of 1198 $mol_{oligomers}\ mol_{Ni}^{-1}\ h^{-1}$, with a selectivity in butene of 54%. Here again polyethylene was observed to be formed around the POP particles.

PAF. Gascon and coworkers proposed the use of Porous Aromatic Frameworks (PAFs) for the oligomerization of ethylene.[134] Three different PAFs were synthesized: two Covalent Triazine Frameworks (CTFs), respectively having a microporous and a mesoporous structure, and one Imine-Linked Porous Organic Network (IL-PON). CTFs exhibit triazine-anchoring sites, which proved to be active when metallated for the ethylene oligomerization. Two different synthetic pathways were used for the synthesis of the three PAFs: by imine-condensation between 2,6-pyridinedicarboxaldehyde and 1,3,5-tris(4-aminophenyl)benzene for the IL-PON PAF and by ionothermal synthesis, with, on one hand 2,6-pyridinedicarbonitrile and $ZnCl_2$ to obtain microporous CTF (microCTF) and on the other hand, 2,6-pyridinedicarbonitrile with 4,4′-biphenyldicarbonitrile and $ZnCl_2$ to synthesize mesoporous CTF (mesoCTF). The materials were metalated afterwards with nickel(II) bromide ethylene glycol dimethyl ether salt ($NiBr_2{\cdot}DME$) in THF, to afford the three catalysts Ni@IL-PON, Ni@meso-CTF and Ni@microCTF. Despite the triazine binding sites, which enable to obtain isolated active sites upon metalation, X-ray photoelectron spectroscopy analysis have revealed the presence of nickel particles physisorbed on the material, which could be responsible for side reactions. Ethylene oligomerization was performed in heptane in a batch reactor, with between 75 and 125 equivalents of Et_3Al during two hours, at 50 °C and under 15 bar of ethylene. The three catalysts Ni@IL-PON, Ni@meso-CTF and Ni@microCTF achieved respectively 92.5, 75.3 and 63 $mol_{ethylene\ converted}\ mol_{Ni}^{-1}\ h^{-1}$, with respective selectivities in butene of 58%, 59% and 54%. Lower TOFs and selectivities are obtained with Ni-based COFs, compared to bpy-based MOFs and POPs.

More recently, Li *et al.* reported two Schiff-base CTF made by condensation of melamine with either 2,3-butanedione, MABD-COF, or p-phthalaldehyde, MAPA-COF.[147] The subsequent metalation with nickel dichloride allowed obtaining two catalysts Ni@MAPA-COF and Ni@MABD-COF with Ni loading of 4.53 wt% and 7.58 wt%, respectively. The coordination of nickel to N atoms from imine-CTF was assessed by FT-IR analysis. The Ni-loaded CTF were evaluated for ethylene oligomerization using MAO as cocatalyst (Al/Ni = 500 to 700) and the best activity were found in cyclohexane as solvent under at 25 °C with a productivity of 7.62×10^4 g $mol_{Ni}^{-1}\ h^{-1}$ and selectivity of 76% for mainly 1-butene using Ni@MABD-COF and a productivity of 15.68×10^4 g $mol_{Ni}^{-1}\ h^{-1}$ and a selectivity of 57% mainly 1-butene using Ni@MAPA-COF. The higher activity of Ni@MAPA-COF was attributed to its larger pore size and accessible surface area compared to Ni@MABD-COF, 192.6 and 6.8 $m^2\ g^{-1}$ respectively, as determined by nitrogen physisorption. The two catalysts were reused three times with a decrease in both the Ni content inside the CTF, indicative for a leaching of active species in the liquid phase, and in the activity, the selectivity remaining the same. In addition, the crystallinity of both catalysts was also altered during the reaction, with a drastic loss of crystallinity for Ni@MABD-COF.

In summary, the literature shows several attempts to obtain very high ethylene oligomerization activity and selectivity towards specific oligomers, by using different methods to obtain isolated active sites. Isolating active sites with materials already containing coordination sites, like bipyridine, present high activity and selectivity towards butenes. However, the side-production of polyethylene remains an issue yet unsolved.

5. Assessing the stability of heterogenized molecular Ni catalysts for reuse

Aiming at high production rate and increased sustainability, the catalyst stability, including both solid integrity and metal leaching, and its subsequent recyclability remains a key issue which can be systematically addressed by assessing the textural, spectroscopic and elemental analyses of the used solid.[128] However, beyond the catalyst integrity, the active site can itself evolve during catalytic runs, leading to a change in reactivity.

In 2015, Farha and coworkers observed that the reuse of NU-1000-bpy-$NiCl_2$ catalyst for a second cycle led to the enhancement of the intrinsic activity for butenes from 1950 to 6040 $mol_{butenes}\ mol_{Ni}^{-1}\ h^{-1}$ with a constant selectivity in butene around 93%.[146] Powder X-Ray diffraction together with the analysis of products and microscopy allowed to evidence that a polymer layer was created around the MOF crystals during the first cycle. The authors assumed that this polymer layer was increasing the local solubility of ethylene during the second cycle at the origin of the enhancement in intrinsic activity for butenes production. When the catalyst was washed carefully with anhydrous ethanol before using it for two more cycles, the observed activity remained the same from 3166 to 2972 $mol_{oligomers}\ mol_{Ni}^{-1}\ h^{-1}$.

In 2017, with the POP-based catalyst Ni(II)-POP-1, Kim *et al.* also confirmed that the ''white insoluble polymer around the POP particles'' was polyethylene.[132] Authors also recovered the

catalyst for two more cycles and, each time, washed it with dichloromethane before activating it under super critical CO_2. Despite the fact that the catalyst remained active for ethylene dimerization, polyethylene continued to cover Ni(II)-POP-1 particles during each cycle, hampering the accessibility of the active sites and hence, decreasing the activity.

Finally, in 2019, Long and coworkers observed that the ethylene consumption of the molecular catalyst $[NiCl_2(bpy)]$ (bpy = 2,2′-bipyridine) and of the MOF $[Ni_3(ndc)_3(DMF)_2\text{-}((CH_3)_2NH)]_n$ (ndc = 2,6-naphtalenedicarboxylate; DMF = *N*,*N*-dimethylformamide), under 10 bars of ethylene at 21 °C, in toluene, with 17 eq. of Et_2AlCl, during one hour, gradually increased in the first minute of each cycle of a five-cycle experiment.[138] This phenomenon was partly attributed to the increasing solubility of ethylene during the recycling experiments due to the presence of oligomers from the previous cycle. In addition, in 2019, Hu *et al.* recycled the Ni-UMOFN catalyst for four consecutive runs, using 10 bars of ethylene at 25 °C, in toluene, with 500 eq. of Et_2AlCl, during one hour, without any significant loss of activity and butene selectivity, by washing the recovered catalyst with dry ethanol before each new cycle.[136]

Thus, in most of the cases reported above, the solid catalyst encountered textural modifications. Most of these modifications occurred during catalysis with polymer formation leading to pore blocking. This detrimental polymerization might be avoided learning lessons from molecular catalysis with better suited combination of active metal and co-catalyst (*i.e.* aluminium salt).[67,148–150] Also large porous system should allow fast diffusion of both C2 reactant and C4 products to limit further reaction towards higher oligomers and polymers. Furthermore, the high confinement of Ni sites in small pores, with strong steric constraints, would reduce the probability for β-H elimination and favour further olefin insertion and, consequently, detrimental pore blocking.[67,76] In addition, layered solids like COF seem less suitable due to their 3D structure collapse through exfoliation under catalytic conditions, concomitant with active site leaching in solution.[151] Indeed, the spacing between sheets within the COF structure might be affected by the growth of interlayered oligomers at the COF-supported nickel sites, leading to a loss of the COF structure.

Finally, at the molecular level, the coordination of nickel single-sites to the porous macroligand might be further tuned. The most reported here are Ni–N species due to the wide availability of N-functionalized building blocks for macroligands, like imidazoles or bipyridines.[17] However, new macroligands based on phosphine and N-heterocyclic carbenes (NHC) should be investigated considering that, in Ni–P, phosphine coordination strength and basicity greatly impacts the selectivity by favouring β-H termination for short oligomers[77] and, in Ni–NHC, stabilization provided by the carbene ligand prevents the catalyst decomposition.[148]

6. Comparing heterogenized molecular catalysts with homogeneous analogues

The embedding of nickel sites into MOFs and POPs macroligands described in the Fig. 6 proved to be an efficient strategy to design heterogeneous catalysts for ethylene oligomerization inspired by molecular counterparts.

However, in self-assembled and cation exchanged Ni-MOF catalysts (routes A and B in the Fig. 6), the Ni–O_2 (from carboxylate) or Ni-N_2 (from imidazolate) species are constitutive of the MOF nodes and relevant comparisons can hardly be made with mono- or dinuclear molecular analogues (Fig. 14, blue). Indeed, a single molecular nickel bis-imidazolate complex, envisioned as analogue for Ni-ZIF MOF, can be hardly compared to an extended MOF structure because the electronic effect of both (i) the two other imidazolates on the nickel and (ii) the second nickel atom coordinated to the imidazolate is impossible to mimic using organic/organometallic functionalization. Considering the atomic deposition (route C in the Fig. 6) using the MOF node as model inorganic surface, the electronic effect of the oxide node on the complex and the effect of the MOF pore microenvironment can also be hardly distinguished. In contrast, supported molecular nickel complexes grafted onto or embedded within the porous network (routes D and E in the Fig. 6) might be more easily compared to homogenous molecular analogues. However the reported heterogenized molecular catalysts often lack comparisons with homogeneous counterparts under the same reaction conditions.[152,153]

In the case of ethylene oligomerization, some of the heterogeneous catalysts developed referred to homogeneous catalysis data previously reported, but often under different conditions.[125,127,131,154] Some other studies compared the catalytic activity of the newly designed heterogeneous catalyst with homogeneous counterparts and under the same conditions (Fig. 14).[128,132,138,146]

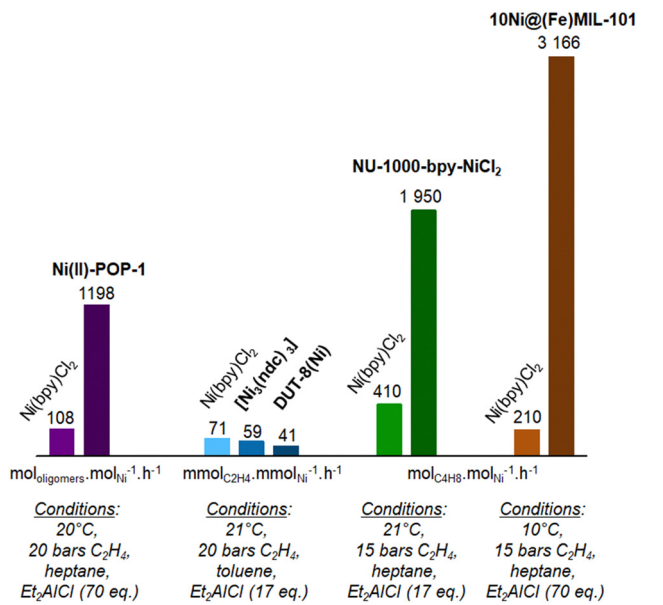

Fig. 14 Comparison of the activity reported for MOF and POP heterogeneous catalysts with homogeneous counterpart for liquid phase ethylene oligomerization under similar conditions: metallatated POP-1 (violet),[132] self-assembled Ni-MOF (blue), and post-synthetically grafted NU-1000 (green)[146] and MIL-101 (brown).[128] Data are given for similar amount of Ni used under mentioned conditions.

The Ni@(Fe)-MIL-101[128] and the Ni(II)-POP-1,[132] respectively a MOF and a POP, proved to be ten times more active than the $Ni(bpy)Cl_2$ molecular complex, under the given conditions.

In the case of Ni@(Fe)-MIL-101, a kinetic model showed that the reaction mechanism of the complex confined within the MOF was similar to that of the molecular complex and included the same elementary steps.[128] According to this kinetic model, there was a small contribution of the solubility of ethylene to the variation of activity as a function of pressure and temperature. The model was based on a reaction mechanism involving the chemisorption of two ethylene molecules on an active nickel site followed by an oligomerization step to 1-butene.

If the choice of organic homogeneous analogue to the MOF and POP solid macroligand is driven by its synthetic or commercial availability, like for bipyridine, a further parameter to be considered is the electronic effect of the organic ligand on the nickel site within the porous solid. Wisser *et al.* demonstrated that the Hammett parameter is an adequate descriptor of electronic effects on the heterogenized molecular active site in the case of rhodium catalysts for reduction reactions in both homogeneous and heterogenized systems.[19,155] The authors showed a linear correlation between the intrinsic catalytic activity and the Hammett parameter calculated for molecular ligands as well as for MOF- and POP-based macroligands, highlighting that the molecular nature of the complexes remained after heterogenization and also the absence of diffusion limitations in the selected solid platforms. For example, organic ester does not account for the same σ value of the Hammett parameter than a zirconium or aluminum carboxylate usually found in bpy-based MOFs. Thus, beyond textural effects due to the confinement into a porous system, the electronic effect of reticulation nodes within porous supports, *i.e.* inorganic units in MOFs or organic bonding in POPs, should not be neglected when comparing MOF and POP catalysts with homogeneous analogues. Such comparison has not been considered in the reported examples.

Diffusion limitations into porous system remain the main aspect addressed – if discussed at all – while comparing homogenous and heterogenized catalysts. In reality, liquid phase/triphasic catalytic systems, such as the case of ethylene oligomerization, implies technical biases that are often not considered such as the local concentration of substrate molecules, especially in the case of different gases solubility between the porous system and the bulk liquid and which will have huge impact on reaction kinetics.

Finally, the most important methodological bias remains the heterogenization of low performing homogeneous catalysts, which is indeed the case of Ni(bpy) species for the ethylene oligomerization, widely studied and discussed here. If a homogeneous catalyst gives outstanding productivity and selectivity, the gain reached by its heterogenization within somehow expensive porous solid becomes much less relevant, even considering its potential recyclability. The immobilization of performing catalysts within a solid porous system thus seems only appealing and valuable if it allows accessing a unique reactivity, impossible to reach in homogeneous phase.

7. Conclusion and perspectives

With the explosion of new families of hybrid porous materials embedding organic ligands for molecular complexes, the heterogenization of molecular catalysts attracts a continuously growing attention. In principle, heterogenized molecular catalyst should benefit for both molecular-level control and advantageous solid-substrate interface interactions. Among catalytic applications, the ethylene oligomerization is a widely and already comprehensively studied reaction in both homogeneous and heterogeneous catalysis and this makes this reaction an example of choice to critically discuss the interest in molecular catalyst heterogenization, as a part of the ever-growing single-site catalyst family.

In the cases summarized here for nickel complexes heterogenization, metal–organic frameworks and porous organic polymers appear to be highly appealing supports because of their high porosity and site density, their infinite variety of design and possible post-synthetic modifications.

For ethylene oligomerization, many MOFs have already been developed, most of them employing Ni as catalytic active site for its high activity and selectivity towards 1-butene. So far, only one bipyridyl-based POP, metallated with a Ni molecular complex, has been developed and tested for ethylene oligomerization. However, a recurrent pitfall is the uncontrolled production of polyethylene, leading to catalyst deactivation.

Beyond obvious technical advantages lying on the easy catalyst separation from the product and its subsequent recycling, the advantages of developing such heterogenized molecular catalysts using sophisticated and costly supports has to be demonstrated. Notwithstanding the wide variety of catalytic conditions reported, this comparison can hardly be done since the organic ligand in the homogeneous complex seldom reproduces the exact same electronic environment as the one in the solid-embedded analogue. Furthermore, the lack of evidence demonstrating the true heterogeneity of the catalysts, particularly from hot filtration and recycling tests, impedes a comprehensive understanding of their nature.

Single-site catalysts, which bridge the gap between homogeneous and heterogeneous catalysis, offer an ideal platform to elucidate the structure–activity relationship using molecular chemistry mechanisms and through the integration of computational chemistry, transient spectroscopy, and advanced diffraction techniques. To facilitate accurate comparison and full comprehension, the geometry of the active site must be unravelled by employing a combination of extensive analytical techniques such as *in situ* X-ray absorption spectroscopy techniques supported by computational chemistry.[156–159] Meanwhile, computational chemistry was demonstrated to be mature enough to give access to molecular mechanisms and even predict reactivity for homogeneous catalysis but is still at its infancy for heterogeneous counterpart.[160] The use of single-site catalyst strategy would allow benefiting from knowledge from homogeneous catalysis while considering the solid support as traditional ligand. However computational methodologies have to be carefully designed on purpose considering the

nature of the support, including rigid organic–inorganic hybrids or highly flexible organic networks.

Finally, an appealing objective of the transfer from homogeneous to heterogeneous phase catalysis is the implementation of heterogenized catalysts in fixed-bed reactor, for either liquid- or gas-phase reactions. However, this often requires prior shaping of the solid catalyst with non-trivial material- and application-dependent strategies in order to avoid critical pressure drop,[161–164] the gas phase testing in fixed-bed reactor being consequently scarcely reported for MOF and POP-based catalysts.[165–167] Even with adequate shaping methodologies linked to gas-phases applications, the fast discovery of high-performing MOF and POP-based catalysts by high-throughput testing remains hindered for sophisticated hybrid solids. One main obstacle in this context is their lab-scale synthesis which offers limited options for upscaling considering their synthetic conditions and associated costs which include raw materials, monomers and metal-based active sites, as well as solvents, often toxic, waste produced and number of synthetic steps.

Thus, the knowledge required to understand and design new generations of heterogenized catalysts could come from the study at the molecular level of the catalyst configuration and interactions at the solid's interface. Moreover, macroscopic behavior plays a crucial role in heterogenous catalysis, making essential to study mechanisms of adsorption, diffusion and kinetics using operando techniques.

This is only by combining the efforts from molecular chemistry, materials science and heterogeneous catalysis that heterogenized molecular catalysis will find its place in today's catalytic processes in order to discover new synthetic pathways while increasing their sustainability.

List of abbreviations

Acac	Acetylacetonate
AFM	Atomic force microscopy
AIM	Atomic layer deposition in MOFs
ALD	Atomic layer deposition
Bdc	1,4-Benzenedicarboxylate
Bipy	Bipyridyl
Bpdc	4,4′-Biphenyldicarboxylate
Bpydc	2,2′-Bipyridine-5,5′-dicarboxylate
COF	Covalent–organic framework
CPO	Coordination polymer of Oslo
CTF	Covalent triazine framework
CVD	Chemical vapor deposition
Dabco	1,4-Diazabicyclo[2.2.2]octane
DFT	Density functional theory
DUT	Dresden University of Technology
Dme	Dimethoxyethane
DMF	*N*,*N*-Dimethylformamide
$Facac^-$	Hexafluoroacetylacetonate
H_2bibtz	1*H*,1′*H*-5,5′-Bibenzo[*d*][1,2,3]triazole
H_2BTDD	Bis(1*H*-1,2,3-triazolo[4,5-*b*],[4′,5′-*i*])dibenzo[1,4]dioxin
ICP-OES	Inductively Coupled Plasma-Optical Emission Spectrometry
IL	Ionic liquids
IL-PON	Imine-linked-porous organic network
IRMOF	IsoReticular MOF
LAO	Linear alpha olefins
MAO	Methylaluminoxanes
MCM	Mobil composition material
MFU	Metal–Organic Framework Ulm-University
MIL	Matériaux of Institut Lavoisier
MMAO	Modified methylaluminoxane
MOF	Metal–organic framework
Ndc	2,6-Naphtalenedicarboxylate
NHC	N-heterocyclic carbene
NMR	Nuclear magnetic resonance
NU	Northwestern University
OPS	One-pot synthesis
PAF	Porous aromatic framework
PCN	Periodic coordination network
PMO	Periodic mesoporous organosilica
POP	Porous organic polymer
PXRD	Powder X-ray diffraction
SAC	Single-atom catalyst
SIM	Solvothermal deposition in MOFs
SOMC	Surface organometallic chemistry
TGA	Thermogravimetric analysis
THF	Tetrahydrofuran
TOF	Turnover frequency
UiO	University of Oslo
UMOFN	Ultrathin metal–organic framework nanosheets
Wt%	Weight percent
ZIF	Zeolite imidazole frameworks

Author contributions

The manuscript was written through contributions of all authors. All authors have given approval to the final version of the manuscript.

Conflicts of interest

There are no conflicts to declare.

Acknowledgements

The authors acknowledge funding from the Agence Nationale de la Recherche, through the grants no. ANR-18-CE07-0025 (Pomac project) and no. ANR-21-CE07-0028 (Flips project), and from the European Union's Horizon 2020 research and innovation program under grant agreement no. 814557 (C123 project). R. R., E. A. Q. and J. C. are thankful to Université Claude Bernard Lyon 1 for R. R. doctoral fellowship.

References

1 B. Pugin, *J. Mol. Catal. A: Chem.*, 1996, **107**, 273–279.

2 C. H. Bartholomew, *Appl. Catal., A*, 2001, **212**, 17–60.
3 J. A. Moulijn, A. E. van Diepen and F. Kapteijn, *Appl. Catal., A*, 2001, **212**, 3–16.
4 A. Z. Fadhel, P. Pollet, C. L. Liotta and C. A. Eckert, *Molecules*, 2010, **15**, 8400–8424.
5 R. H. Crabtree, *Chem. Rev.*, 2015, **115**, 127–150.
6 C. Copéret, A. Comas-Vives, M. P. Conley, D. P. Estes, A. Fedorov, V. Mougel, H. Nagae, F. Núñez-Zarur and P. A. Zhizhko, *Chem. Rev.*, 2016, **116**, 323–421.
7 C. Copéret, *Acc. Chem. Res.*, 2019, **52**, 1697–1708.
8 M. D. Korzyński and C. Copéret, *Trends Chem.*, 2021, **3**, 850–862.
9 S. R. Docherty, L. Rochlitz, P.-A. Payard and C. Copéret, *Chem. Soc. Rev.*, 2021, **50**, 5806–5822.
10 C. Copéret, Z. J. Berkson, K. W. Chan, J. de, J. Silva, C. P. Gordon, M. Pucino and P. A. Zhizhko, *Chem. Sci.*, 2021, **12**, 3092–3115.
11 M. K. Samantaray, E. Pump, A. Bendjeriou-Sedjerari, V. D'Elia, J. D. A. Pelletier, M. Guidotti, R. Psaro and J.-M. Basset, *Chem. Soc. Rev.*, 2018, **47**, 8403–8437.
12 J.-M. Basset, F. Lefebvre and C. Santini, *Coord. Chem. Rev.*, 1998, **178–180**, 1703–1723.
13 C. Copéret and J.-M. Basset, *Adv. Synth. Catal.*, 2007, **349**, 78–92.
14 C. Copéret, M. Chabanas, R. Petroff Saint-Arroman and J.-M. Basset, *Angew. Chem., Int. Ed.*, 2003, **42**, 156–181.
15 J. M. Basset and A. Choplin, *J. Mol. Catal.*, 1983, **21**, 95–108.
16 P. Avenier, M. Taoufik, A. Lesage, X. Solans-Monfort, A. Baudouin, A. de Mallmann, L. Veyre, J.-M. Basset, O. Eisenstein, L. Emsley and E. A. Quadrelli, *Science*, 2007, **317**, 1056–1060.
17 F. M. Wisser, Y. Mohr, E. A. Quadrelli and J. Canivet, *ChemCatChem*, 2020, **12**, 1270–1275.
18 F. M. Wisser, P. Berruyer, L. Cardenas, Y. Mohr, E. A. Quadrelli, A. Lesage, D. Farrusseng and J. Canivet, *ACS Catal.*, 2018, **8**, 1653–1661.
19 F. M. Wisser, Y. Mohr, E. A. Quadrelli, D. Farrusseng and J. Canivet, *ChemCatChem*, 2018, **10**, 1778–1782.
20 F. M. Wisser, Y. Mohr, E. A. Quadrelli and J. Canivet, *ChemCatChem*, 2020, **12**, 1270–1275.
21 S. Daliran, A. R. Oveisi, Y. Peng, A. López-Magano, M. Khajeh, R. Mas-Ballesté, J. Alemán, R. Luque and H. Garcia, *Chem. Soc. Rev.*, 2022, **51**, 7810–7882.
22 T. Drake, P. Ji and W. Lin, *Acc. Chem. Res.*, 2018, **51**, 2129–2138.
23 A. Dhakshinamoorthy, A. M. Asiri and H. Garcia, *ChemCatChem*, 2020, **12**, 4732–4753.
24 S. Abednatanzi, M. Najafi, P. Gohari Derakhshandeh and P. Van Der Voort, *Coord. Chem. Rev.*, 2022, **451**, 214259.
25 A. H. Chughtai, N. Ahmad, H. A. Younus, A. Laypkov and F. Verpoort, *Chem. Soc. Rev.*, 2015, **44**, 6804–6849.
26 S. M. J. Rogge, A. Bavykina, J. Hajek, H. Garcia, A. I. Olivos-Suarez, A. Sepúlveda-Escribano, A. Vimont, G. Clet, P. Bazin, F. Kapteijn, M. Daturi, E. V. Ramos-Fernandez, F. X. L. i Xamena, V. V. Speybroeck and J. Gascon, *Chem. Soc. Rev.*, 2017, **46**, 3134–3184.
27 Y. Zhang and S. N. Riduan, *Chem. Soc. Rev.*, 2012, **41**, 2083–2094.
28 A. Alimardanov, L. Schmieder-van de Vondervoort, A. H. M. de Vries and J. G. de Vries, *Adv. Synth. Catal.*, 2004, **346**, 1812–1817.
29 C. Deraedt and D. Astruc, *Acc. Chem. Res.*, 2014, **47**, 494–503.
30 L. Kuai, Z. Chen, S. Liu, E. Kan, N. Yu, Y. Ren, C. Fang, X. Li, Y. Li and B. Geng, *Nat. Commun.*, 2020, **11**, 48.
31 A. S. Galushko, D. A. Boiko, E. O. Pentsak, D. B. Eremin and V. P. Ananikov, *J. Am. Chem. Soc.*, 2023, **145**, 9092–9103.
32 Z. Li, N. M. Schweitzer, A. B. League, V. Bernales, A. W. Peters, A. ''Bean'' Getsoian, T. C. Wang, J. T. Miller, A. Vjunov, J. L. Fulton, J. A. Lercher, C. J. Cramer, L. Gagliardi, J. T. Hupp and O. K. Farha, *J. Am. Chem. Soc.*, 2016, **138**, 1977–1982.
33 V. Bernales, A. B. League, Z. Li, N. M. Schweitzer, A. W. Peters, R. K. Carlson, J. T. Hupp, C. J. Cramer, O. K. Farha and L. Gagliardi, *J. Phys. Chem. C*, 2016, **120**, 23576–23583.
34 J. Canivet, E. Bernoud, J. Bonnefoy, A. Legrand, T. K. Todorova, E. A. Quadrelli and C. Mellot-Draznieks, *Chem. Sci.*, 2020, **11**, 8800–8808.
35 H.-Y. Zhuo, X. Zhang, J.-X. Liang, Q. Yu, H. Xiao and J. Li, *Chem. Rev.*, 2020, **120**, 12315–12341.
36 A. Nandy, H. Adamji, D. W. Kastner, V. Vennelakanti, A. Nazemi, M. Liu and H. J. Kulik, *ACS Catal.*, 2022, **12**, 9281–9306.
37 M. K. Samantaray, V. D'Elia, E. Pump, L. Falivene, M. Harb, S. Ould Chikh, L. Cavallo and J.-M. Basset, *Chem. Rev.*, 2020, **120**, 734–813.
38 A. K. Datye and H. Guo, *Nat. Commun.*, 2021, **12**, 895.
39 S. Mitchell and J. Pérez-Ramírez, *Nat. Commun.*, 2020, **11**, 4302.
40 X.-F. Yang, A. Wang, B. Qiao, J. Li, J. Liu and T. Zhang, *Acc. Chem. Res.*, 2013, **46**, 1740–1748.
41 I. B. Moroz, A. Lund, M. Kaushik, L. Severy, D. Gajan, A. Fedorov, A. Lesage and C. Copéret, *ACS Catal.*, 2019, **9**, 7476–7485.
42 Z. Chen, S. R. Docherty, P. Florian, A. Kierzkowska, I. B. Moroz, P. M. Abdala, C. Copéret, C. R. Müller and A. Fedorov, *Catal. Sci. Technol.*, 2022, **12**, 5861–5868.
43 S. Hübner, J. G. de Vries and V. Farina, *Adv. Synth. Catal.*, 2016, **358**, 3–25.
44 G. P. Belov and P. E. Matkovsky, *Pet. Chem.*, 2010, **50**, 283–289.
45 O. L. Sydora, *Organometallics*, 2019, **38**, 997–1010.
46 P. Cossee, *Tetrahedron Lett.*, 1960, **1**, 12–16.
47 E. J. Arlman, *J. Catal.*, 1964, **3**, 89–98.
48 J. Petit, L. Magna and N. Mézailles, *Coord. Chem. Rev.*, 2022, **450**, 214227.
49 R. Robinson, D. S. McGuinness and B. F. Yates, *ACS Catal.*, 2013, **3**, 3006–3015.
50 R. Y. Brogaard and U. Olsbye, *ACS Catal.*, 2016, **6**, 1205–1214.

51 U. Müller, W. Keim, C. Krüger and P. Betz, *Angew. Chem., Int. Ed. Engl.*, 1989, **28**, 1011–1013.
52 V. P. Ananikov, *ACS Catal.*, 2015, **5**, 1964–1971.
53 S. Z. Tasker, E. A. Standley and T. F. Jamison, *Nature*, 2014, **509**, 299–309.
54 J. Yamaguchi, K. Muto and K. Itami, *Eur. J. Org. Chem.*, 2013, 19–30.
55 E. Richmond and J. Moran, *Synthesis*, 2018, 499–513.
56 S. Bhakta and T. Ghosh, *Adv. Synth. Catal.*, 2020, **362**, 5257–5274.
57 N. Hazari, P. R. Melvin and M. M. Beromi, *Nat. Rev. Chem.*, 2017, **1**, 1–16.
58 K. S. Egorova and V. P. Ananikov, *Angew. Chem., Int. Ed.*, 2016, **55**, 12150–12162.
59 V. P. Ananikov, D. G. Musaev and K. Morokuma, *Organometallics*, 2005, **24**, 715–723.
60 S. A. Macgregor, G. W. Neave and C. Smith, *Faraday Discuss.*, 2003, **124**, 111–127.
61 L. K. Johnson, C. M. Killian and M. Brookhart, *J. Am. Chem. Soc.*, 1995, **117**, 6414–6415.
62 C. M. Killian, D. J. Tempel, L. K. Johnson and M. Brookhart, *J. Am. Chem. Soc.*, 1996, **118**, 11664–11665.
63 C. Wang, S. Friedrich, T. R. Younkin, R. T. Li, R. H. Grubbs, D. A. Bansleben and M. W. Day, *Organometallics*, 1998, **17**, 3149–3151.
64 T. R. Younkin, E. F. Connor, J. I. Henderson, S. K. Friedrich, R. H. Grubbs and D. A. Bansleben, *Science*, 2000, **287**, 460–462.
65 D. P. Gates, S. A. Svejda, E. Oñate, C. M. Killian, L. K. Johnson, P. S. White and M. Brookhart, *Macromolecules*, 2000, **33**, 2320–2334.
66 P.-A. R. Breuil, L. Magna and H. Olivier-Bourbigou, *Catal. Lett.*, 2015, **145**, 173–192.
67 H. Olivier-Bourbigou, P. A. R. Breuil, L. Magna, T. Michel, M. F. Espada Pastor and D. Delcroix, *Chem. Rev.*, 2020, **120**, 7919–7983.
68 J. Diccianni, Q. Lin and T. Diao, *Acc. Chem. Res.*, 2020, **53**, 906–919.
69 T. Sperger, I. A. Sanhueza, I. Kalvet and F. Schoenebeck, *Chem. Rev.*, 2015, **115**, 9532–9586.
70 J.-B. Liu, X. Wang, A. M. Messinis, X.-J. Liu, R. Kuniyil, D.-Z. Chen and L. Ackermann, *Chem. Sci.*, 2021, **12**, 718–729.
71 R. Lhermet, E. Moser, E. Jeanneau, H. Olivier-Bourbigou and P.-A. R. Breuil, *Chem. – Eur. J.*, 2017, **23**, 7433–7437.
72 F. Speiser, P. Braunstein and L. Saussine, *Inorg. Chem.*, 2004, **43**, 4234–4240.
73 G. Wilke, B. Bogdanović, P. Hardt, P. Heimbach, W. Keim, M. Kröner, W. Oberkirch, K. Tanaka, E. Steinrücke, D. Walter and H. Zimmermann, *Angew. Chem., Int. Ed. Engl.*, 1966, **5**, 151–164.
74 W. Keim, F. H. Kowaldt, R. Goddard and C. Krüger, *Angew. Chem., Int. Ed. Engl.*, 1978, **17**, 466–467.
75 D. H. Camacho and Z. Guan, *Chem. Commun.*, 2010, **46**, 7879–7893.
76 M. Peuckert and W. Keim, *Organometallics*, 1983, **2**, 594–597.
77 P. Kuhn, D. Sémeril, D. Matt, M. J. Chetcuti and P. Lutz, *Dalton Trans.*, 2007, 515–528.
78 U. Klabunde, R. Mulhaupt, T. Herskovitz, A. H. Janowicz, J. Calabrese and S. D. Ittel, *J. Polym. Sci., Part A: Polym. Chem.*, 1987, **25**, 1989–2003.
79 G. Wilke, *Angew. Chem., Int. Ed. Engl.*, 1988, **27**, 185–206.
80 W. Keim, *Angew. Chem., Int. Ed. Engl.*, 1990, **29**, 235–244.
81 A. Finiels, F. Fajula and V. Hulea, *Catal. Sci. Technol.*, 2014, **4**, 2412–2426.
82 M. Lallemand, O. A. Rusu, E. Dumitriu, A. Finiels, F. Fajula and V. Hulea, *Appl. Catal., A*, 2008, **338**, 37–43.
83 M. Lallemand, O. A. Rusu, E. Dumitriu, A. Finiels, F. Fajula and V. Hulea, *Studies in Surface Science and Catalysis*, Elsevier, 2008, vol. 174, pp. 1139–1142.
84 R. D. Andrei, E. Borodina, D. Minoux, N. Nesterenko, J.-P. Dath, C. Cammarano and V. Hulea, *Ind. Eng. Chem. Res.*, 2020, **59**, 1746–1752.
85 Y. Chen, E. Callens, E. Abou-Hamad, N. Merle, A. J. P. White, M. Taoufik, C. Copéret, E. Le Roux and J.-M. Basset, *Angew. Chem., Int. Ed.*, 2012, **51**, 11886–11889.
86 A. Hamieh, R. Dey, B. Nekoueishahraki, M. K. Samantaray, Y. Chen, E. Abou-Hamad and J.-M. Basset, *Chem. Commun.*, 2017, **53**, 7068–7071.
87 Y. Chen, R. Credendino, E. Callens, M. Atiqullah, M. A. Al-Harthi, L. Cavallo and J.-M. Basset, *ACS Catal.*, 2013, **3**, 1360–1364.
88 J. M. Basset and A. Choplin, *J. Mol. Catal.*, 1983, **21**, 95–108.
89 C. Copéret, F. Allouche, K. W. Chan, M. P. Conley, M. F. Delley, A. Fedorov, I. B. Moroz, V. Mougel, M. Pucino, K. Searles, K. Yamamoto and P. A. Zhizhko, *Angew. Chem., Int. Ed.*, 2018, **57**, 6398–6440.
90 P. Van Der Voort, D. Esquivel, E. De Canck, F. Goethals, I. Van Driessche and F. J. Romero-Salguero, *Chem. Soc. Rev.*, 2013, **42**, 3913–3955.
91 C. T. Kresge, M. E. Leonowicz, W. J. Roth, J. C. Vartuli and J. S. Beck, *Nature*, 1992, **359**, 710–712.
92 D. Y. Shin, J. H. Yoon, H. Baik and S. J. Lee, *Appl. Catal., A*, 2020, **590**, 117363.
93 A. Aid, R. D. Andrei, S. Amokrane, C. Cammarano, D. Nibou and V. Hulea, *Appl. Clay Sci.*, 2017, **146**, 432–438.
94 M. Fallahi, E. Ahmadi and Z. Mohamadnia, *Appl. Organomet. Chem.*, 2019, **33**, e4975.
95 A. Al Khudhair, K. Bouchmella, R. D. Andrei, A. Mehdi, P. H. Mutin and V. Hulea, *Microporous Mesoporous Mater.*, 2021, **322**, 111165.
96 Y.-S. Wei, M. Zhang, R. Zou and Q. Xu, *Chem. Rev.*, 2020, **120**, 12089–12174.
97 D. Farrusseng, S. Aguado and C. Pinel, *Angew. Chem., Int. Ed.*, 2009, **48**, 7502–7513.
98 J. Lee, O. K. Farha, J. Roberts, K. A. Scheidt, S. T. Nguyen and J. T. Hupp, *Chem. Soc. Rev.*, 2009, **38**, 1450–1459.
99 J. Liu, L. Chen, H. Cui, J. Zhang, L. Zhang and C.-Y. Su, *Chem. Soc. Rev.*, 2014, **43**, 6011–6061.
100 T. Zhang and W. Lin, in *Metal-Organic Frameworks for Photonics Applications*, ed. B. Chen and G. Qian, Springer, Berlin, Heidelberg, 2014, pp. 89–104.

101 Y. Wen, J. Zhang, Q. Xu, X.-T. Wu and Q.-L. Zhu, *Coord. Chem. Rev.*, 2018, **376**, 248–276.
102 R. J. Kuppler, D. J. Timmons, Q.-R. Fang, J.-R. Li, T. A. Makal, M. D. Young, D. Yuan, D. Zhao, W. Zhuang and H.-C. Zhou, *Coord. Chem. Rev.*, 2009, **253**, 3042–3066.
103 C. Xu, R. Fang, R. Luque, L. Chen and Y. Li, *Coord. Chem. Rev.*, 2019, **388**, 268–292.
104 L. Ma, C. Abney and W. Lin, *Chem. Soc. Rev.*, 2009, **38**, 1248–1256.
105 J.-X. Jiang, F. Su, A. Trewin, C. D. Wood, N. L. Campbell, H. Niu, C. Dickinson, A. Y. Ganin, M. J. Rosseinsky, Y. Z. Khimyak and A. I. Cooper, *Angew. Chem., Int. Ed.*, 2007, **46**, 8574–8578.
106 J.-S. M. Lee and A. I. Cooper, *Chem. Rev.*, 2020, **120**, 2171–2214.
107 A. G. Slater and A. I. Cooper, *Science*, 2015, **348**, aaa8075.
108 A. Thomas, F. Goettmann and M. Antonietti, *Chem. Mater.*, 2008, **20**, 738–755.
109 D. Taylor, S. J. Dalgarno, Z. Xu and F. Vilela, *Chem. Soc. Rev.*, 2020, **49**, 3981–4042.
110 F. Vilela, K. Zhang and M. Antonietti, *Energy Environ. Sci.*, 2012, **5**, 7819–7832.
111 K. Sakaushi and M. Antonietti, *Acc. Chem. Res.*, 2015, **48**, 1591–1600.
112 P. Kaur, J. T. Hupp and S. T. Nguyen, *ACS Catal.*, 2011, **1**, 819–835.
113 Q. Sun, Z. Dai, X. Meng, L. Wang and F.-S. Xiao, *ACS Catal.*, 2015, **5**, 4556–4567.
114 C. Mellot-Draznieks and A. K. Cheetham, *Nat. Chem.*, 2017, **9**, 6–8.
115 P. Mialane, C. Mellot-Draznieks, P. Gairola, M. Duguet, Y. Benseghir, O. Oms and A. Dolbecq, *Chem. Soc. Rev.*, 2021, **50**, 6152–6220.
116 J. Sauer, *Acc. Chem. Res.*, 2019, **52**, 3502–3510.
117 Y. J. Colón and R. Q. Snurr, *Chem. Soc. Rev.*, 2014, **43**, 5735–5749.
118 R. Dawson, A. I. Cooper and D. J. Adams, *Prog. Polym. Sci.*, 2012, **37**, 530–563.
119 Y. Tian and G. Zhu, *Chem. Rev.*, 2020, **120**, 8934–8986.
120 K. T. Tan, S. Ghosh, Z. Wang, F. Wen, D. Rodríguez-San-Miguel, J. Feng, N. Huang, W. Wang, F. Zamora, X. Feng, A. Thomas and D. Jiang, *Nat. Rev. Methods Primers*, 2023, **3**, 1–19.
121 A. P. Côté, A. I. Benin, N. W. Ockwig, M. O'Keeffe, A. J. Matzger and O. M. Yaghi, *Science*, 2005, **310**, 1166–1170.
122 M. J. Bojdys, J. Jeromenok, A. Thomas and M. Antonietti, *Adv. Mater.*, 2010, **22**, 2202–2205.
123 P. Kuhn, M. Antonietti and A. Thomas, *Angew. Chem., Int. Ed.*, 2008, **47**, 3450–3453.
124 P. Kuhn, A. Forget, J. Hartmann, A. Thomas and M. Antonietti, *Adv. Mater.*, 2009, **21**, 897–901.
125 C. Chen, M. R. Alalouni, X. Dong, Z. Cao, Q. Cheng, L. Zheng, L. Meng, C. Guan, L. Liu, E. Abou-Hamad, J. Wang, Z. Shi, K.-W. Huang, L. Cavallo and Y. Han, *J. Am. Chem. Soc.*, 2021, **143**, 7144–7153.
126 E. D. Metzger, R. J. Comito, Z. Wu, G. Zhang, R. C. Dubey, W. Xu, J. T. Miller and M. Dincă, *ACS Sustainable Chem. Eng.*, 2019, **7**, 6654–6661.
127 E. D. Metzger, C. K. Brozek, R. J. Comito and M. Dincă, *ACS Cent. Sci.*, 2016, **2**, 148–153.
128 J. Canivet, S. Aguado, Y. Schuurman and D. Farrusseng, *J. Am. Chem. Soc.*, 2013, **135**, 4195–4198.
129 B. Liu, S. Jie, Z. Bu and B.-G. Li, *RSC Adv.*, 2014, **4**, 62343–62346.
130 L. Chen, Y. Jiang, H. Huo, J. Liu, Y. Li, C. Li, N. Zhang and J. Wang, *Appl. Catal., A*, 2020, **594**, 117457.
131 M. I. Gonzalez, J. Oktawiec and J. R. Long, *Faraday Discuss.*, 2017, **201**, 351–367.
132 M. J. Kim, S. Ahn, J. Yi, J. T. Hupp, J. M. Notestein, O. K. Farha and S. J. Lee, *Catal. Sci. Technol.*, 2017, **7**, 4351–4354.
133 K. Kyogoku, C. Yamada, Y. Suzuki, S. Nishiyama, K. Fukumoto, H. Yamamoto, S. Indo, M. Sano and T. Miyake, *J. Jpn. Pet. Inst.*, 2010, **53**, 308–312.
134 E. Rozhko, A. Bavykina, D. Osadchii, M. Makkee and J. Gascon, *J. Catal.*, 2017, **345**, 270–280.
135 U. S. F. Arrozi, V. Bon, S. Krause, T. Lübken, M. S. Weiss, I. Senkovska and S. Kaskel, *Inorg. Chem.*, 2020, **59**, 350–359.
136 Y. Hu, Y. Zhang, Y. Han, D. Sheng, D. Shan, X. Liu and A. Cheng, *ACS Appl. Nano Mater.*, 2019, **2**, 136–142.
137 U. S. F. Arrozi, V. Bon, C. Kutzscher, I. Senkovska and S. Kaskel, *Dalton Trans.*, 2019, **48**, 3415–3421.
138 U. S. F. Arrozi, V. Bon, C. Kutzscher, I. Senkovska and S. Kaskel, *Dalton Trans.*, 2019, **48**, 3415–3421.
139 N. Guillou, C. Livage, M. Drillon and G. Férey, *Angew. Chem., Int. Ed.*, 2003, **42**, 5314–5317.
140 C. Wang, G. Li and H. Guo, *Mol. Catal.*, 2022, **524**, 112340.
141 C. Chen, M. R. Alalouni, P. Xiao, G. Li, T. Pan, J. Shen, Q. Cheng and X. Dong, *Ind. Eng. Chem. Res.*, 2022, **61**, 14374–14381.
142 E. D. Metzger, R. J. Comito, Z. Wu, G. Zhang, R. J.-C. Dubey, W. Xu, J. T. Miller and M. Dinca, *ACS Sustainable Chem. Eng.*, 2019, **7**, 6654–6661.
143 J. Liu, J. Ye, Z. Li, K. Otake, Y. Liao, A. W. Peters, H. Noh, D. G. Truhlar, L. Gagliardi, C. J. Cramer, O. K. Farha and J. T. Hupp, *J. Am. Chem. Soc.*, 2018, **140**, 11174–11178.
144 B. Yeh, S. P. Vicchio, S. Chheda, J. Zheng, J. Schmid, L. Löbbert, R. Bermejo-Deval, O. Y. Gutiérrez, J. A. Lercher, C. C. Lu, M. Neurock, R. B. Getman, L. Gagliardi and A. Bhan, *J. Am. Chem. Soc.*, 2021, **143**, 20274–20280.
145 S. Bauer, C. Serre, T. Devic, P. Horcajada, J. Marrot, G. Férey and N. Stock, *Inorg. Chem.*, 2008, **47**, 7568–7576.
146 S. T. Madrahimov, J. R. Gallagher, G. Zhang, Z. Meinhart, S. J. Garibay, M. Delferro, J. T. Miller, O. K. Farha, J. T. Hupp and S. T. Nguyen, *ACS Catal.*, 2015, **5**, 6713–6718.
147 D. Li, L. Guo, F. Li, J. Huang, J. Li, M. Li and C. Li, *Microporous Mesoporous Mater.*, 2022, **338**, 111979.
148 D. S. McGuinness, W. Mueller, P. Wasserscheid, K. J. Cavell, B. W. Skelton, A. H. White and U. Englert, *Organometallics*, 2002, **21**, 175–181.

149 D. E. Ortega, D. Cortés-Arriagada, O. S. Trofymchuk, D. Yepes, S. Gutiérrez-Oliva, R. S. Rojas and A. Toro-Labbé, *Chem. – Eur. J.*, 2017, **23**, 10167–10176.
150 K. N. Tayade, M. V. Mane, S. Sen, C. N. Murthy, G. L. Tembe, S. M. Pillai, K. Vanka and S. Mukherjee, *J. Mol. Catal. A: Chem.*, 2013, **366**, 238–246.
151 Y. Tao, W. Ji, X. Ding and B.-H. Han, *J. Mater. Chem. A*, 2021, **9**, 7336–7365.
152 Q. Sun, Z. Dai, X. Meng, L. Wang and F.-S. Xiao, *ACS Catal.*, 2015, **5**, 4556–4567.
153 U. I. Kramm, R. Marschall and M. Rose, *ChemCatChem*, 2019, **11**, 2563–2574.
154 E. D. Metzger, R. J. Comito, Z. Wu, G. Zhang, R. C. Dubey, W. Xu, J. T. Miller and M. Dincă, *ACS Sustainable Chem. Eng.*, 2019, **7**, 6654–6661.
155 F. M. Wisser, P. Berruyer, L. Cardenas, Y. Mohr, E. A. Quadrelli, A. Lesage, D. Farrusseng and J. Canivet, *ACS Catal.*, 2018, **8**, 1653–1661.
156 N. M. Sackers, A. Iemhoff, P. Sautet and R. Palkovits, *Catal. Sci. Technol.*, 2023, **13**, 2652–2655.
157 N. V. Velthoven, S. Waitschat, S. M. Chavan, P. Liu, S. Smolders, J. Vercammen, B. Bueken, S. Bals, K. P. Lillerud, N. Stock and D. E. D. Vos, *Chem. Sci.*, 2019, **10**, 3616–3622.
158 A. Zitolo, V. Goellner, V. Armel, M.-T. Sougrati, T. Mineva, L. Stievano, E. Fonda and F. Jaouen, *Nat. Mater.*, 2015, **14**, 937–942.
159 A. Zitolo, N. Ranjbar-Sahraie, T. Mineva, J. Li, Q. Jia, S. Stamatin, G. F. Harrington, S. M. Lyth, P. Krtil, S. Mukerjee, E. Fonda and F. Jaouen, *Nat. Commun.*, 2017, **8**, 957.
160 J. P. Reid and M. S. Sigman, *Nat. Rev. Chem.*, 2018, **2**, 290–305.
161 S. Das, T. Ben and S. Qiu, *Polymer*, 2020, **207**, 122928.
162 A. Abramova, N. Couzon, M. Leloire, P. Nerisson, L. Cantrel, S. Royer, T. Loiseau, C. Volkringer and J. Dhainaut, *ACS Appl. Mater. Interfaces*, 2022, **14**, 10669–10680.
163 Y. Khabzina, J. Dhainaut, M. Ahlhelm, H.-J. Richter, H. Reinsch, N. Stock and D. Farrusseng, *Ind. Eng. Chem. Res.*, 2018, **57**, 8200–8208.
164 B. Yeskendir, J.-P. Dacquin, Y. Lorgouilloux, C. Courtois, S. Royer and J. Dhainaut, *Mater. Adv.*, 2021, **2**, 7139–7186.
165 C. Wang, B. An and W. Lin, *ACS Catal.*, 2019, **9**, 130–146.
166 R. A. Peralta, M. T. Huxley, J. D. Evans, T. Fallon, H. Cao, M. He, X. S. Zhao, S. Agnoli, C. J. Sumby and C. J. Doonan, *J. Am. Chem. Soc.*, 2020, **142**, 13533–13543.
167 D. P. Zhuchkov, M. V. Nenasheva, M. V. Terenina, Yu. S. Kardasheva, D. N. Gorbunov and E. A. Karakhanov, *Pet. Chem.*, 2021, **61**, 1–14.

